The political economy of socioenvironmental conflict: Evidence from Peru*

David Kreitmeir†

Monash University

(Click here for the latest version)

November 9, 2023

Abstract

This study uses a unique and fine-grained data set on social conflict events in Peru and exogenous variation in world mineral prices to show that a surge in projected local mineral rents increases the probability of violent confrontations between protesters and national police. A 10% increase in the main mineral price has no effect on protester riots, but leads to a 1.9-percentage-point increase in the probability of injuries among protesters and a 0.7-percentage-point increase in the probability of a protester being killed. I provide evidence suggestive of political capture of the judicial process. I show that the likelihood of initial investigations being undertaken against narrowly elected pro-mining mayors for corruption offenses in office is significantly lower than that for anti-mining candidates while the chance of formal charges being levied against the former is elevated. Finally, I provide suggestive evidence for the efficacy of police violence in forestalling official conflict resolution agreements that acknowledge protesters' demands.

Keywords: Resource curse, mining, social conflicts, local authorities, Peru

JEL Codes: D74, H7, O13, O16, P16, Q34.

*I thank Sascha O. Becker, Paul A. Raschky, Thomas Ueberfuhr, Alexander Ballantyne, and the SoDa Labs PhD group as well as participants of the Melbourne PolEcon/PolSci meeting and the 13th Australasian Public Choice Conference for their helpful suggestions and comments.

†Monash University, Department of Economics, 900 Dandenong Rd, Caulfield East, VIC 3145, Australia. Email: david.kreitmeir1@monash.edu.

1 Introduction

Over the last two decades, the blessing and curse of mineral resource endowments has been on display in Peru. Having enjoyed an impressive mining boom since the start of this century, with yearly mineral rents reaching up to 600 US dollars (USD) per capita, Peru has seen a coincident rise in social conflicts related to formal mining.[1] From March 2004 to December 2019, more than 386 anti-mining activists were injured and at least 41 killed in demonstrations against expropriation of local lands and allegedly inadequate compensation for environmental damages by formal mining companies.[2] This pattern is not isolated to Peru: it is part of a worrying global trend of endemic violence against socioenvironmental activists besetting even stable democracies such as Peru.[3] However, this form of conflict has so far received relatively little attention in the resource curse literature, which has mainly focused on armed civil conflict, particularly rebel insurgencies fueled by natural resource rents in Africa (Berman et al., 2017; Sánchez De La Sierra, 2020) and South America (Dube and Vargas, 2013). Panel A in Figure 1 graphically illustrates this positive relationship between natural resource rents and armed civil conflict: countries with above-median natural resource rents experienced more casualties related to armed civil conflict over the 2002–2019 period. Focusing on this set of countries, Panel B in Figure 1 juxtaposes the number of killed environmental defenders over this period with the number of civil conflict fatalities, revealing the (relative) prevalence and severity of socioenvironmental conflicts even in democracies.

Utilizing a unique granular data set on violence against protesters during socioenvironmental conflicts in Peru and exogenous variation in monthly world mineral prices, this paper provides new empirical evidence on the causal relationship between mineral rents and violence in socioenvironmental conflicts: a projected rise in local mineral rents is estimated to increase the likelihood of both nonfatal and fatal violence against protesters

[1]Figure A.2 in the appendix provides a graphical illustration.

[2]These figures are the author's calculations based on reports published by the Peruvian Office of the ombudsman.

[3]Peru exhibited a *Polity2* score (Marshall et al., 2002) of 9 (of a maximum 10 and a minimum -10) throughout the period from 2002 to 2019. In relative terms, Peru's *Polity2* score equaled that of France over this period and surpassed that of the United States from 2016 to 2019.

opposing mining projects.

Peru's institutional framework provides a unique setting to shed light on the nexus between mineral rents and the suppression of socioenvironmental protests. Local governments in Peru are highly dependent on central government transfers because of their limited ability to levy and collect taxes. Two of the most lucrative transfers available to district governments are based on local mining activity. According to a fixed allocation rule, the central government transfers 50% of income taxes collected from mining companies and 80% of royalties to local governments in mining regions. While recent studies have shown that this redistribution scheme can positively affect human capital accumulation (Agüero et al., 2021) and living standards in mining districts (Loayza and Rigolini, 2016), it can also create adverse incentives for local authorities to suppress local opposition to mining projects. Further, in the presence of political capture, democratic institutions might fail to align the incentives of local communities and politicians.

In this paper, I combine information on mineral production and concessions at the district level with social conflict events to test the hypothesis that an increase in mineral rents raises the likelihood of violence against activists during socioenvironmental protests. My identification strategy relies on exogenous changes in world mineral prices to estimate the effect of expected changes in mineral rents on protest suppression. I find that a spike in mineral prices increases the probability of observing protester arrests, injuries and deaths during confrontations with the national police (PNP).Leveraging the spatial and temporal granularity of the data set, I conduct the analysis at the month and district level, where the district is the third and lowest administrative level in Peru. By conditioning on district $\times$ year fixed effects, I account for time-varying and time-invariant district characteristics that potentially confound the estimated relationship, such as changes to the funds available to local governments from mining revenues. I show that the estimated relationship between mineral rents and violence against protesters cannot be explained by more militant behavior on the side of activists. Moreover, the benchmark estimates are robust to the exclusion of confrontations with protester violence and across numerous sensitivity tests.

Having documented how changes in expected mineral rents affect the use of force against protesters, I turn to the role of mayors, who are in charge of local security. Using a regression discontinuity design (RDD), I test whether the election of a pro-mining as opposed to an anti-mining candidate increases the probability of excessive use of force against activists and corruption in the district. For this question, I collect a new data set on mayoral government plans published ahead of elections. Using natural language processing (NLP) and large language models (LLMs), I label over 9,000 candidates on the basis of their revealed sentiment toward formal mining activities in published government plans. I find suggestive evidence in support of the hypothesis that the marginal election of a pro-mining candidate has a positive estimated effect on violence against protesters during her time in office. Further, the RDD results are indicative of political capture in the judicial process. Using information on the procedural stage of corruption cases against former mayors, I show that pro-mining mayors have a significantly lower probability of facing initial investigations against them. However, once only cases that lead to formal charges or sentences are considered, corruption is—if anything—more likely during a pro-mining candidate's than an anti-mining candidate's mayoral term, suggesting that investigations are misappropriated as a political tool against marginally elected anti-mining candidates.[4]

In the last part of the paper, I provide suggestive evidence for the efficacy of police violence in dispersing protests. Exploiting unique information on the evolution of social conflicts over time in the data set, I use a marginal structural model (MSM) framework (Blackwell, 2014; Imai and Ratkovic, 2015) to estimate the dynamic causal effect of violence against activists on the final outcome of the social conflict. In particular, I find that the probability that local communities receive financial compensation, as proxied by the signing of an official resolution agreement, decreases if excessive force is used against protesters. I show that the effect is qualitatively robust across different estimation algorithms and models.

[4]This is in line with the finding of Bland and Chirinos (2014) and Artiles et al. (2021) that recall elections in Peru are used as a political tool by runner-ups to oust elected mayors from office prior to the end of their term.

This study relates to various strands of the literature. By moving the focus from armed conflict over the appropriation of natural resources to socioenvironmental conflict, the study contributes to the rich empirical literature on the nexus between natural resource abundance and local conflict (Dube and Vargas, 2013; Berman et al., 2017; Sánchez De La Sierra, 2020, among others). Using exogenous variation in world mineral prices, Berman et al. (2017) show that a surge in mineral rents increases the probability of conflict at the local level in Africa. The authors highlight the importance of mineral resources in financing insurgency activities of rebel groups. The central role of revenues from natural resource extraction is underlined in recent work by Sánchez De La Sierra (2020), who documents that rebel groups in the Democratic Republic of the Congo establish quasi-states around mines. Along the same lines, Dube and Vargas (2013) show that positive oil price shocks increase paramilitary attacks in oil-producing municipalities. I complement the existing results by presenting new empirical evidence on the causal relationship between mineral rents and the violent suppression of opposition to local mining projects.

The study's results align with findings from a growing strand of literature that has started to explore the determinants of social conflict and related violence (Haslam and Ary Tanimoune, 2016; Castellares et al., 2017; Butt et al., 2019; Sexton, 2020; Grasse, 2022). Haslam and Ary Tanimoune (2016) combine information on the location of mining properties in South America and hand-coded data on social conflicts to provide the first solid empirical foundation for the hypothesized causes of social conflict, which, until their work, had been based on qualitative findings and case-study evidence (e.g., Bebbington et al., 2008; Arellano-Yanguas, 2011; Arce, 2014). The authors find that economic grievances in local communities and property characteristics, such as foreign ownership, are positively correlated with the emergence of social conflicts. A more recent literature has started to address the issue of causal identification. Grasse (2022) shows that palm oil price shocks lead to more confrontations between current landowners and prospective producers in Indonesia. Sexton (2020) documents that a surge in mineral prices leads to more social conflict incidents related to highly visible pollution in Peruvian departments but not for less observable environmental degradation. The present study augments these findings by utilizing the spatial and temporal granularity of the data to causally identify the effect of changes in mineral rents on local social conflicts by relying exclusively on within-district–year variation. Detailed information on protest events, moreover, allows me to discern whether the violence against activists is the result of more militant behavior on the side of activists or is indeed generated by excessive use of force by the police.

This paper also contributes to the literature on the redistribution of natural resource rents and the effect of mining activity on local communities and politics. For the case of Peru's *canon minero*—a fiscal transfer scheme of mining revenues—Maldonado and Ardanaz (2022) document a positive but nonmonotonic effect of additional funds in the hands of local governments on human capital accumulation, while Loayza and Rigolini (2016) and Aragón and Rud (2013) document improvements in the standard of living for local communities. On the other hand, the literature has found the *canon minero* to be associated with higher levels of corruption (Maldonado, 2011) and inefficient use of public funds (Maldonado, 2017). This is in line with the finding of Baragwanath Vogel (2021) that windfall gains in oil-producing municipalities in Brazil lead to higher levels of corruption. An increase in local corruption with the advent of local mining activity is, moreover, documented by Knutsen et al. (2017) for Africa. For India, Asher and Novosad (2023) show that local mining booms increase criminal politicians' likelihood of being elected and committing crimes in office. The present paper's results dovetail with this work on the adverse effects of mining activity on local communities, highlighting violence against activists as an important negative externality. Furthermore, the paper provides evidence of political capture of the judicial process in relation to mining activity.

Finally, the paper makes a methodological contribution. To the best of my knowledge, it is the first to use the marginal structural model (MSM) framework to causally identify how violence affects the outcome of conflicts. The model, originally developed by Robins et al. (2000), was introduced to the social sciences by Blackwell (2014). Using this empirical framework, he was able to identify a causal effect of negative campaigns in the lead-up to U.S. elections on the vote share. The method has since been applied and refined by, among others, Imai and Ratkovic (2015), Montgomery and Olivella (2018), and Bodory et al. (2022).

2 Mineral Rents and Social Conflict Violence

2.1 Institutional Framework

Peru has three administrative levels, with groups of districts (*distritos*) forming provinces (*provincias*) and groups of provinces forming regions (*departamentos*). In 2001, as part of a fiscal decentralization reform, the national government implemented a fiscal transfer scheme—the so-called *canon minero*—which distributes 50% of the income taxes collected from mining corporations back to local governments according to a fixed allocation rule. In particular, since the enactment of of Law No. 28327 in 2004, 10% of this amount is directly distributed to producing districts; 20% of the amount is shared among all districts in a producing province, and 40% is distributed among all districts in a producing region. In addition, Law No. 28258 in 2004 established that 20% of the collected mining royalties are directly transferred to the district(s) where the mining concession is located, 20% are distributed among districts in the province of the mining concession, and 40% are allocated to districts in the region of the concession.[5] Table A.2 in the appendix presents summary statistics for the amount of total revenues in real 2010 USD received by districts from either the *canon minero* or royalties over the period 2004 to 2020. Additionally, the total revenues are disaggregated by district category, i.e., whether a district had mining production, only concessions but no active production, or neither during the sample period. Table A.2 illustrates the favorable position of mineral-producing districts and the substantial financial incentives for local governments to attract mining projects. In particular, local governments are highly dependent on fiscal transfers from the central government, with the share of the *canon minero* accounting for approximately 29% of local governments' budgets and as much as 70% of those of producing districts (Canavire-

[5]With the exception of the 10% of the *canon minero* and the 20% of the mining royalties directly transferred to districts, the exact allocation of *canon* transfers and royalties to districts is determined by social and economic characteristics in the respective district.

Bacarreza et al., 2012; Maldonado and Ardanaz, 2022).[6] While the use of funds received from the *canon minero* or royalties is tied to specified objectives, the limited impact of transfers on living standards has been connected to corruption and unproductive but politically favorable investments in local infrastructure and public employment (Maldonado, 2011; Crabtree, 2014; Maldonado, 2017). In particular, the electoral system, which grants the elected mayor 50%-plus-one seats in the district council independent of the election results, has severely limited political accountability in the absence of a strong civil society (Maldonado, 2011; Crabtree, 2014).

2.2 Data

2.2.1 Social Conflicts

For this study, I construct a unique data set of social conflicts related to mining projects in Peru based on reports by the Office of the ombudsman (*Defensoría del Pueblo*), henceforth referred to as "the ombudsman."[7] Since April 2004, the ombudsman has published monthly reports on social conflicts in Peru. These reports follow a fairly uniform format, which enables me to identify and track developments of individual social conflicts over time. In particular, each report entry constitutes a separate social conflict and contains the following key information: type of social conflict, location, actors, current status (active, latent, resolved or removed) and a description of recent events related to the conflict if any transpired.[8] An example entry is presented in Figure A.1 in the appendix.

I restrict the set of social conflicts for this study to conflicts concerning industrial mining. Therefore, I exclude conflicts related to informal or illegal mining activities to account for fundamental differences in the characteristics of these conflicts. In particular, the latter often take place in regions with no official mining production and—by

[6]The dependence of local governments on central transfers in Peru is the result of their marginal ability to levy and collect taxes, with self-raised revenues contributing on average only 12.5% to the local budget (Aresti, 2016).

[7]Other empirical studies have used ombudsman reports for information on social conflict incidence (Arellano-Yanguas, 2011; Haslam and Ary Tanimoune, 2016; Castellares et al., 2017; Orihuela et al., 2019; Sexton, 2020, among others). To the best of my knowledge, no studies so far, however, have used the social conflict data at such fine-grained spatial and temporal resolution.

[8]If a conflict is inactive (latent) for an extended period of time, the ombudsman removes the case from the register.

definition—involve actors more prone to using illegal means to secure mining rents. While a role of local authorities as stakeholders in these illegal operations cannot be ruled out, the concern of this study is the "visible" suppression of mining opposition by the PNP, which operates under the direction of local governments. Further, I require that an industrial mining entity be one of the primary actors in the conflict. Note that this set of conflicts also comprises unfulfilled promises about employment for local community members in exchange for licensing their land but excludes labor disputes about inadequate pay, dangerous working conditions.

The baseline sample is, moreover, confined to social conflicts with location information at the district level to identify whether and how changes in local mineral rents lead to escalations in local anti-mining conflicts. The resulting data set is an unbalanced panel at the conflict–month level over the March 2004 to December 2015 period, with the first observation for each conflict being the month when the conflict first enters the ombudsman's register.

Further, I create an accompanying data set on protest activities against mining corporations on basis of the description of recent events in the ombudsman reports. In particular, I code the date if specified and if not the month of the protest, the location of the event, and the number of injuries, arrests, and casualties among protesters. For cases in which the exact number of injuries or arrests is not clearly specified, the number is coded as one to provide a conservative estimate. I aggregate all variables to the monthly level to match the frequency of social conflict reports and rely on binary coding of all protest measures in the empirical analysis.

For the baseline analysis, I use the granular information on locations of protests and social conflicts to construct a balanced panel of social conflicts and their associated protests at the district–month level for the period from March 2004 to December 2015. I supplement these data with a revised version of Kreitmeir et al.'s (2020) data set on the killings of activists. In particular, this data set covers a longer time period from 1998 to 2020 and comprises assassinations of mining activists outside of protests that are not covered in the ombudsman reports.

2.2.2 Mineral Production and Prices

I obtain data on monthly mineral production disaggregated by type of mineral at the district level from the Ministry of Energy and Mining (MINEM) for the period from 2002 to 2019.[9] I combine the information on mineral production with monthly world prices on minerals provided by the *World Bank*. The *World Bank Commodity Price Data* cover seven minerals that represent more than 99% of the total production value over this period.[10] All mineral prices are uniformly expressed as real USD per kilogram.

Following Berman et al. (2017), I determine the main mineral in a district on the basis of its total production value over the period 2002–2019 evaluated at mineral prices at the start of the period 2002. As an alternative price measure, I construct a weighted price index of all minerals mined in a district, with weights equal to each mineral's share in total production value in the district over the 2002–2019 period.

For my baseline estimations, I additionally consider the presence of mining concessions in a district. Data on mining claims are drawn from the *SNL Mining & Metals* database. Anecdotal evidence from the ombudsman suggests that social conflicts often break out before the production stage, when a mining concession is granted. In conjunction with royalty revenues being based on concession location rather than production value, an analysis relying exclusively on mineral production might not capture the "total" effect of changes in mineral rents on the violent suppression of activists. Figure 2 illustrates this nexus. A substantial share of the social conflicts associated with industrial mining are located in districts with no mineral production during the study period. However, in many of these districts, mining concessions—visualized by white rectangular areas framed in black—were granted during this time. Figures A.3 and A.4 in the appendix provide analogous images for mining royalties and *canon minero* distributed to each district during the 2002–2019 period. Since information on the selling price or projected

[9]Note that MINEM also provides production data for the year 2001. However, the data are available only at the departmental level. For more details, see: http://www.minem.gob.pe/_estadistica.php?idSector=1&idEstadistica=12501.

[10]The minerals are iron, copper, lead, tin, zinc, gold, and silver. Price timelines for each of those minerals are presented in Figure A.6 in the appendix. Price changes in the top 75th (90th) percentile are depicted in blue (red). Note that I collect prices at the yearly level for the remainder of minerals mined in Peru from the USGS. For more details on mineral prices, see Appendix Section A.3.

value of concessions is not available in the *SNL Mining & Metals* database, I determine the main mineral for a nonproducing district on the basis of a simple count of each concession's primary commodity. For weighted price index, the weights are calculated based on the primary commodity counts of each mineral for the granted concessions in the district.

Table 1 provides descriptive statistics for the main variables of interest disaggregated by presence of mining production or concessions. The total data set comprises 1873 districts over 18 years; 228 districts had a positive production value over the 2002–2019 period, with 278 additional districts granting at least one mining concession. The probability of observing the violent death of an activist or use of force against activists in a district in a given month is between 0.01% and 0.04%. The likelihood of observing any of these events more than quadruples when I consider only districts with mining production. An increase in the average probability of observing protester arrests or injuries is also observed for districts with mining concessions granted during the study period.

2.2.3 Other Data

I obtain data on *canon minero* and mining royalty transfers from the Ministry of Economy and Finance (MEF).[11] I convert all yearly transfer payments into real USD using the official yearly exchange rate and MUV Index provided by the *World Bank*. Information on administrative boundaries is retrieved from the National Institute of Statistics and Information Technology (INEI).[12]

[11]The MEF makes the data publicly available through its Transparency Portal (*Transparencia Económica*), which can be accessed here:https://apps5.mineco.gob.pe/transferencias/gl/default.aspx.

[12]The data can be accessed here: https://www.datosabiertos.gob.pe/dataset/resource/a43e17c8-fa37-463d-aa7e-2ce2a272491b.

2.3 Empirical Strategy

Leaning on the empirical framework in Berman et al. (2017), the baseline linear probability model (LPM) takes the form:

$$A_{it} = \delta \left(M_i \times \ln(P_{it}^W) \right) + \mathbf{X}_{it}'\beta + \gamma_{iy} + \epsilon_{it}, \tag{1}$$

where A_{it} takes on the value one if a forceful action against protesters is taken by the police force (or vice versa) in month t in district i and 0 otherwise. M_i equals one if there has been *(i)* mineral production and for the baseline specification if *(ii)* a mining concession was granted in district i during the period 2002–2019 and equals zero otherwise. My use of a constant mining indicator variable accounts for potential reverse causality. In particular, local opposition to a mining project could lead to a halt in production or the withdrawal of the mining concession. Holding the production indicator fixed ensures that the coefficient of interest δ is identified by exogenous movements in world mineral prices only.

The inclusion of district $\times$ year fixed effects, γ_{iy}, accounts for time-invariant district characteristics simultaneously affecting social conflict and local mining activity such as property rights enforcement or historical disenfranchisement of indigenous communities. My focusing exclusively on within-district–year variation, moreover, lets me control for time-varying differences across districts at the yearly level, in particular economic and budgetary changes in municipalities. P_{it}^W denotes the world price of the *main* mineral in district i. For districts with no mining production (or districts with no concessions), the mineral price is set to zero. For my baseline estimates, the main mineral in a district is the mineral with either the highest total production value (in 2002 USD prices) or the highest primary commodity count among granted concessions. I test the robustness of my results derived with the baseline price variable to my use of an alternative value-weighted price index. In particular, this price index is the value-weighted price of all minerals mined in district i over the 2002–2019 period, with weights equaling the production value in producing districts. For nonproducing concession districts, the weights are determined on basis of the number of primary commodities of granted concessions in the district. Additionally, I test the sensitivity of my baseline estimates to my restricting the sample to only producing districts. $\mathbf{X}_{it}$ is a set of potential time-varying codeterminants of social conflict that I consider in robustness checks.

Given the granularity of the data and the spatial clustering of events, the standard errors are allowed to be spatially and temporally correlated. Specifically, I correct the standard errors for heteroskedasticity and autocorrelation (HAC), retaining a radius of 500 km for the spatial kernel.[13] I assume a linear decay in distance for the spacial correlation for nonzero elements in the HAC matrix.[14] Serial correlation is allowed to be "unconstrained" and can span the entire sample period. I also provide robustness results for alternative spatial radii.

2.4 Baseline Results

Table 2 presents the results for three baseline social conflict incidents involving use of force against activists during public protests by the PNP.[15] I estimate that a one-percentage-point increase in the main mineral price increases the probability of protesters' being arrested by 0.04 percentage points, of their being injured by 0.19 percentage points, and of their being killed by 0.07 percentage points. These effects are sizable. Relative to the mean, a one-percentage-point increase in mineral prices more than doubles the probability of my observing use of excessive force.

Having established a positive relationship between projected mineral rents and use of force against protesters, columns 4 and 5 test whether the observed escalation of social conflicts is indeed the result of a harsher crackdown by the PNP or can be explained by more militant behavior on activists' side provoking a reaction from police. While the conflicts under investigation are concerned with environmental and social issues related to mining activity and not the appropriation of mineral resources as considered in the civil conflict literature (Berman et al., 2017), frustrations over insufficient compensation

[13]The radius of 500 km is taken as it is close to the median internal distance of 540 km.

[14]In detail, the nonzero elements of the HAC spatial pattern matrix follow a Bartlett kernel (Colella et al., 2023).

[15]In rare instances, private security guards are involved in the confrontations.

for environmental damage or properties might surge among protesters when the expected rents for mining corporations and local authorities increase. To address this potential channel, I use information on injuries and killings of police officers during demonstrations to create a binary indicator that equals one if violence against police forces is observed and zero if otherwise. Note that this variable could also capture acts of retaliation at the hands of protesters in response to initial violence by police. The estimated effect might hence overstate the impact of changes in mineral rents on protester violence.

Reassuringly, I find no evidence for an effect of mineral prices on protester violence (column 5 in Table 2). The estimated effect, moreover, remains quantitatively stable and insignificant if I additionally consider other forms of militant behavior such as property destruction (column 5).

In summary, the baseline findings provide evidence for the hypothesis that a surge in (expected) mineral rents leads to a harsher and more violent crackdown on protesters but does not significantly affect vandalism or violence among protesters.

2.5 Robustness Checks

This subsection explores the sensitivity of the baseline results in several dimensions.

2.5.1 Omitted Variables

In the first set of robustness checks, I address concerns about potential omitted variables.

Neighborhood analysis Leaning on Berman et al. (2017), I implement a neighborhood fixed effects regression model. For this specification, I define the "control set" for each mining district as comprising the first- and second-degree neighboring *nonmining* districts. Each mining district and its neighbors form a "neighborhood group," with the price of the main mineral in the *mining* district also assigned to its neighbors. I include neighborhood $\times$ year fixed effects to absorb any constant and time-varying codeterminants of social conflict and mining activity across neighborhoods. Any identifying variation in this model derives from the differential reaction to price shocks between mining districts and their inactive neighbors.

Table 3 presents the estimates for the neighborhood fixed effects model. The estimated probability of observing protest suppression by police forces is significantly higher in mining districts, while no significant difference for protester violence and riots is visible. The results are qualitatively stable when I consider the ten nearest neighbors by distance (Table B.1 in the appendix).

Time-varying covariates In Table B.2 in the appendix, I additionally control for district-specific factors varying at the monthly level that have been identified in the literature to be associated with conflict probability such as agricultural commodity prices (Dube and Vargas, 2013; Berman and Couttenier, 2015; McGuirk and Burke, 2020) and weather conditions (Hsiang et al., 2013; Harari and Ferrara, 2018). Movements in these variables could coincide with mineral price shocks and protest incidences. First, I introduce the main crop price in a district as an additional control. Following the coding of the main mineral price, the former is the agricultural commodity in a district with the highest production value. To calculate the total production value, I combine world commodity prices from the *World Bank* with crop-specific agricultural land cover circa 2000 from the *M3-Cropland* project (Monfreda et al., 2008).[16] The effect of crop prices is estimated to be indistinguishable from zero, while mineral prices retain their positive and significant coefficient. Similarly, the coefficient of interest remains statistically and quantitatively stable with the inclusion of temperature and rainfall as controls.

2.5.2 Measurement

Section B.2 in the appendix shows that the baseline findings are robust to my considering alternative definitions and measures of *(i)* the district-specific mineral price, *(ii)* protest incidence, and *(iii)* mining activity.

Price index First, I investigate the robustness of the baseline results to the use of the price of all minerals mined in a district aggregated into a price index in lieu of

[16] The M3 crops data are also used by Berman and Couttenier (2015), Harari and Ferrara (2018), and McGuirk and Burke (2020), among others.

the main mineral price. The price index is calculated as the weighted average price of all mined minerals, with the time-constant weights defined as the mineral's share of the total production value in a district over the sample period. The robust coefficient estimates for the alternative price measure are presented in Table B.3.

Outcomes Second, I check the sensitivity of the baseline estimates to the definition of protest incidence. In column 1 of Table B.4, I consider not only casualties during protests but also slayings of activists outside of protests and by unknown perpetrators. The coefficient estimate remains positive but declines in magnitude and is no longer significantly different from zero. The prolonged planning process involved in assassinations, hence, appears to make them less susceptible to short-term price fluctuations.

Furthermore, the exclusion of events with "unconfirmed" details—i.e., incidences where the number of injuries or arrests is not clearly stated—or months with coinciding protester riots have little effect on the magnitude and significance of the estimated effect.

Table B.5 in the appendix presents estimates for the baseline specification when I use the location of the social conflict associated with a protest incident in lieu of the event location. That is, the protest incident is now coded as if it had happened in all districts spanned by the corresponding social conflict. While this alternative outcome definition leads to an (expected) loss of precision in the estimates, the magnitude of the effects remains quantitatively stable.

Production districts Third, I restrict the sample to districts with at least one year of mineral production. Districts with mining concessions but no production during the sample period are, hence, disregarded. Table B.6 in the appendix shows that the focus on production districts results in larger but less precisely estimated coefficients. However, all coefficients of interest remain significant at at least the 10% level.

2.5.3 Econometric Specification

The baseline specification uses the the log of the level of the mineral price and does not consider potential temporal or spatial lags.

Level vs. first difference The use of price levels has evolved as the standard in the conflict literature (Berman et al., 2017, 2019) but requires that the price series be stationary. Unit root tests for each mineral-specific monthly price series (once purged from their common time components) suggest that the price series are stationary, with the exception of that of monthly gold prices, for which the null hypothesis of the presence of a unit root marginally cannot be rejected at the 10% level (Figure B.1). To alleviate potential misspecification concerns, I present in Tables B.7 and B.8 in Section B.3 of the appendix the estimates for the change in the natural logarithm of the main mineral price and the price index, respectively, from month $t-1$ to t. This focus on price growth results in qualitatively similar but less precisely estimated effects.

Temporal and spatial lags Further, allowing for spatial spillovers increases the impact of mineral prices (Table B.9), whereas including temporal lags B.10 has little influence on the cumulative effect. The results align with findings on spatial lags in the civil conflict literature (Berman et al., 2017; McGuirk and Burke, 2020; Berman et al., 2019).

2.5.4 Additional Robustness Checks

World market share A potential concern with the proposed identification strategy is that social conflicts could impact mineral production to such an extent that they have some influence on world prices. Table A.3 in the appendix presents in Panel A the world share of Peruvian mineral production disaggregated by mineral and year and in Panel B the corresponding maximum share among all districts. While Panel A confirms Peru's position as one of the main global mineral producers, Panel B illustrates that, with the exception of tin, no district has a world share above 5%, making any world prices movements for those minerals plausibly exogenous.[17] To check for the possibility that local social conflicts affect world mineral pries, I drop all districts whose world market share ever exceeded 1% during the sample period from 2004 to 2019 for this analysis.[18]

[17]The San Rafael mine is located in the district of Antauta, in the province of Melgar, in the region of Puno.

[18]Applying the 1% threshold is equivalent to excluding districts in the 90th percentile of world market share among all producing districts.

Table B.11 in the appendix shows that the coefficients are virtually unchanged from the benchmark estimates, alleviating concerns about a potential violation of the exogeneity assumption.

Standard errors Next, I provide robustness results for different spatial kernels. In particular, I allow for unlimited serial correlation and spatial correlation within a radius of up to 50 km, 100 km, 250 km, 500 km, 750 km, and 1,000 km. For both dimensions, I assume a linear decay in distance. Table B.12 in the appendix presents standard error estimates for these alternative levels of clustering. The estimates for protester arrests, injuries, and deaths retain significance at the 5% level regardless of which spatial radius is used, while the estimates for protester behavior remain indistinguishable from zero.

Multiple-hypothesis correction Finally, I address concerns that my baseline findings could suffer from an overrejection of the null hypotheses as a result of reuse of the identifying exogenous variation for multiple outcomes. I apply the *Romano–Wolf* multiple-hypothesis correction procedure, described in Romano and Wolf (2005a,b, 2016) and implemented by Clarke et al. (2020), to safeguard against false rejection of true null hypotheses. In recent work, Heath et al. (2022) show that the employed method performs well in a multitude of settings and across different dimensions. Table B.13 in the appendix presents for each baseline outcome variable the original model p-value, the resampled p-value from 500 bootstraps, and the *Romano–Wolf* p-value corrected for multiple hypothesis testing.[19] The estimates for arrests, injuries, and the fatal use of force against protesters remain significant at the 10% level once multiple hypothesis testing is explicitly controlled for, while the null hypothesis of no effect of mineral rents on protester behavior cannot be rejected at common thresholds.

[19] A graphical illustration of the null distributions used to calculate the *Romano–Wolf* adjusted p-values for each of the five baseline outcome variables is given in Figure B.2 in the appendix.

3 Mechanisms

3.1 Democracy, Corruption, and Violence

In this section, I examine the how the elections of pro-mining politicians affects police violence against protesters and corruption during time in office.

3.1.1 Data

I combine data from various sources to build a municipality–candidate-level data set.

Data on election outcomes are obtained from the National Jury of Elections (JNE) online database Infogob. This includes the list of mayoral candidates and the results of municipal elections for 2002, 2006, 2010, 2014, and 2018. In addition, I obtain information on recall referenda for these five rounds of municipal elections to determine whether a sitting mayor was recalled prior to the end of her term.

Infogob also publishes government plans ("*planes de gobierno*") of candidates for each election round, with the exception of 2010.[20] These provide unique information on the political program and ideology of mayoral candidates against the background of highly fragmented and candidate-centered local-level politics in Peru (Bland and Chirinos, 2014; Artiles et al., 2021).[21] I scraped government plans from the website to assemble a novel and comprehensive data set on the (stated) stance of candidates on formal mining activity. In particular, I classify candidates based on their government plans as *anti-mining*, *pro-mining* or *neutral* toward formal mining. The classification procedure can be summarized in the following steps. First, I preprocess the documents to obtain the raw text and use a semiautomatically derived mining keyword list to filter out passages concerned with formal mining. All government plans that do not contain any mining keywords are classified as "unknown." Next, I use OpenAI's large language model *GPT-4* to answer five questions based on the passages extracted in the previous step to determine a candidate's sentiment toward formal mining. Note that a candidate's being classified as *anti-mining*

[20] While links to government reports for elections in 2010 are provided on the government website, these links cannot be accessed, and the browser returns an error message (last accessed 6 October 2023).

[21] For instance, Artiles et al. (2021) report that, of the average 7.26 candidates running for mayor in 2014, only 36.9% ran for a national party.

does not require the candidate to oppose formal mining entirely; a focus on constraining current mining practices or on the negative environmental impacts of mining suffices. If the answers exhibit any inconsistencies, e.g., if the GPT-4 answers indicate a focus on both the positive and negative impacts of mining, I feed the text back to GPT-4 with a verification question to resolve the conflict.[22] Appendix Section A.2 provides a detailed discussion on the classification process.

Data on corruption are retrieved from the PPEDC's 2022 report on corruption in regional and local governments (Pacheco Palacios et al., 2022).[23] Importantly, the report not only lists cases for which a former mayor has been sentenced for crimes against public administration (e.g., abuse of power, embezzlement, collusion, etc.) but also cases still at the investigative stage. Following the procedural model of the PPEDC, I group cases into three procedural stages: the early investigative stage ("*investigación preparatoria*"), the second intermediate stage ("*etapa intermedia*") when formal charges are brought or dropped by the prosecutor, and the final trial stage ("*juzgamiento*").[24]

In line with the baseline analysis, the final sample is restricted to municipalities with mineral production or concessions during the 2002–2019 period. Moreover, the sample is restricted to 234 mayoral races with either a pro- or an anti-mining candidate's victory in the election.[25]

3.1.2 Empirical Strategy

If local authorities are indeed able to (illegally) extract rents from mining transfers and profit from mining expansions, we should observe higher levels of corruption and violence against mining opponents during the terms of pro-mining mayors than during the terms

[22]If the classification procedure returns an error at any of the stages, I resort to manual labeling of the government plan.

[23]In particular, I obtain information on the procedural stage of the case, the name of the accused, and the category of the crimes committed against public administration from Section 7 p. 209–613.

[24]For more details on the procedural stages, please refer to page 18 of Pacheco Palacios et al. (2022).

[25]While a simple pro-mining and *not pro-mining* candidate RDD is possible, such an analysis suffers from the very noisy signal of governments plans that either do not discuss formal mining activity at all or exhibit a neutral sentiment toward it. Without clearly stated preferences, government plans cannot serve as a prediction of behavior in office. Unreported results show that the inclusion of races with marginal losses and wins by *not pro-mining* candidates introduces a substantial amount of noise, resulting in imprecise estimates.

of mayors who plan on restricting mining activity. However, the victory of a pro-mining candidate is plausibly correlated with a broad range of municipality characteristics, including the historic prevalence of corruption. In return, corruption itself might be determined by municipality characteristics. For instance, unexploited mineral reserves might attract mining corporations willing to make illegal payments to secure a certification of the environmental impact study required for production.

To overcome these identification challenges, I employ an RDD. Using the margin of victory—defined as the difference between the vote percentage obtained by the first pro-mining candidate and the first anti-mining candidate—as the running variable, I take advantage of the discontinuity in the assignment to treatment between the victory of a pro- as opposed to an anti-mining mayor. The treatment assignment mechanism is:

$$L_i = \begin{cases} L_i = 1 & \text{if } x_i > 0 \\ L_i = 0 & \text{if } x_i < 0, \end{cases} \tag{2}$$

where x_i denotes the margin of victory of the pro-mining candidate and L_i reflects the treatment status and equals 1 if a pro-mining candidate won the election.

The corresponding regression model takes the form:

$$y_i = \delta_0 + \delta_1 L_i + \delta_2 f(x_i) + \delta_3 L_i \times f(x_i) + \epsilon_i, \tag{3}$$

where y_i represents the outcome and $f(x_i)$ is a polynomial function of the margin of victory. Finally, ϵ_i denotes the idiosyncratic error term.

The coefficient of interest, δ_1, captures the estimated effect of (narrowly) electing a pro-mining candidate as opposed to an anti-mining candidate. For δ_1 to be correctly identified, two key assumptions have to be fulfilled: (1) there should be no manipulation around the cut-off, and (2) covariates potentially correlated with both the treatment and outcome variables should not significantly differ around the cut-off. On the former, the manipulation test based on density at the discontinuity as suggested by Cattaneo et al. (2018) is presented in Figure C.1 in the appendix and provides no evidence of systematic manipulation around the cut-off. On the latter, Table C.1 in the appendix shows that municipality characteristics are not significantly different around the threshold.

I follow Cattaneo et al. (2020) and estimate the RDD specified in Equation 3 non-parametrically using polynomials of order 1 and 2 and triangular kernel weights. The optimal bandwidth is chosen to minimize the asymptotic mean squared error (MSE). I report robust standard errors adjusted for clustering at the state level (Calonico et al., 2014; Cattaneo et al., 2020).

3.1.3 Results

Figure 3 presents the effect of electing a pro-mining mayor on police violence and corruption during her time in office. The left and right columns display estimates using linear and quadratic polynomial approximations, respectively. Table C.2 presents the results in greater detail.

Panel A shows a positive jump around the threshold for observing at least one incident of police violence against protesters during the term of a pro-mining as opposed to an anti-mining mayor. While the magnitude of the estimated effect is sizable, with an increase of over 150% over the average probability of observing police violence, limited variation in the outcome variable renders the point estimates narrowly insignificant, with a p-value of approximately 13% (columns 1 and 2 of Table C.2).

An interesting pattern arises when we look at corruption crimes during the time in office. Panel B of Figure 3 suggest that the victory of a pro-mining decreases—albeit not significantly—the probability of corruption in office. However, Panel B disguises interesting heterogeneity across procedural stages of corruption cases. Panel C shows a clear discontinuous drop in the probability of corruption cases at the investigative stage (*stage 1*) around the cut-off, while Panel D suggests that, when only corruption cases at least at the intermediary stage with formal chargers are considered, the victory of a pro-mining as opposed to an anti-mining candidate is—if anything—associated with higher levels of corruption. The observed pattern is consistent with political capture of the investigative process. The marginal election of an anti-mining candidate appears to trigger significantly more investigations against a mayor, but these cases appear to not lead to formal chargers or sentences—the stages at which we expect the influence of pro-mining candidates over the judicial process to be lower.

3.2 Is Use of Excessive Force Effective?

In this section, I take advantage of a unique feature of the social conflict data set: each social conflict and associated events are tracked over time. This allows me to investigate whether the violent suppression of social protests proves effective (from the perspective of the repressing authorities). To causally identify the effect of interest, I apply a marginal structural model (MSM) framework.

3.2.1 Data

The end of social conflicts can be broadly categorized into three different outcomes: *(1)* signing of a resolution agreement *(2)* "removal" of the conflict due to inactivity, and *(3)* right-censoring of the conflict due to the end of the study period. For this analysis, I focus on comparing the former two outcomes. In particular, *resolution* agreements usually contain some form of concession to the activists such as compensation payments for the (illegal) use of communal land or damages to the environment; they are costly for mining corporations and local authorities and, therefore, can serve as a proxy for an "undesired" outcome from their point of view. In contrast, the *removal* of a conflict from the list of social conflicts tracked by the ombudsman requires a period of prolonged inactivity. This outcome can, hence, be viewed as "desirable" and "costless" (conditional on conflict length).

Note that I define the end of the conflict as the last month when the social conflict was still active. This definition allows me to account for two aspects of the data. First, the Peruvian ombudsman does not have a fixed threshold of duration of inactivity beyond which social conflicts are no longer tracked; i.e., conflicts can be removed after 8 months of inactivity or two years. Second, some social conflicts become inactive after the successful negotiation of a resolution agreement but before its signing.

I combine the data on social conflicts with an extensive set of time-varying and time-invariant conflict-specific covariates. The set of time-varying controls comprises past incidents of police violence, protests and protester riots as well as information on mineral and crop prices, rainfall or temperature. The set of time-invariant covariates includes district characteristics such as night light, share of indigenous lands, mining transfers, and conflict characteristics such as the the market capitalization and location of the majority owner of the mining project associated with the conflict. Table A.1 in the appendix provides a comprehensive list of all variables.

3.2.2 Dynamic Causal Inference

The causal identification of the effect of interest in this setting requires the use of dynamic causal inference methods. Traditional methods that fail to account for the dynamic process preceding the final outcome will face a dilemma—failing to include important covariates leads to *omitted variable bias*—but the inclusion of these covariates might coincidentally introduce *post-treatment bias*.

To make things less abstract, consider the following illustrative example. Following consecutive months of protests, local authorities decide to use excessive force to disperse the opposition. On the one hand, failing to account for past protest incidents would result in omitted variable bias. On the other hand, police violence might spark more protests in return, triggering a harsher crackdown. Including protests as a covariate would, hence, lead to *post-treatment bias.*[26]

As originally shown in Robins et al. (2000) and later by Blackwell (2014), *marginal structural models* (MSMs) using *inverse probability of treatment weighting* (IPTW) on the data allow causal identification in the present setting if two main assumptions are fulfilled: *sequential ignorability* and *positivity.* Intuitively, sequential ignorability requires that, conditional on the covariate and action (treatment) history, social conflicts experiencing violent suppression at a particular time t are "similar" to those that do not.[27] Second, the

[26]Figure D.2 in the appendix visualizes this dynamic causal framework.

[27]Figure D.3 in the appendix provides a graphical illustration of a scenario when the sequential ignorability assumption is fulfilled (Panel A) and when it is violated (Panel B).

assumption of positivity requires that all action sequences that are theoretically possible be observed in the data.[28] Since months with police violence are rare events, I recode the data such that a single time period t encompasses 3 months. [29] Moreover, I follow Blackwell (2013) and restrict the analysis to common support on baseline covariates, which in essence defaults to the exclusion of time periods that never experienced police violence across conflicts from the analysis.

Intuitively, IPTW works because actions—here police violence—become unrelated to the measured confounders in the reweighted data and, thus, confounders can no longer explain any remaining differences between action sequences. Formally, suppose that there are $i = 1, ..., N$ social conflicts, each spanning $t = 1, ..., T_i$ 3-month periods, where T_i denotes the last 3-month period of conflict i and $t = 1$ the "baseline" time period—i.e., the time period before the social conflict begins. In each time period of the conflict, we observe whether local authorities decide to use force against opponents, denoted $A_{it} = 1$, or abstain from such measures ($A_{it} = 0$). At the same time, the circumstances around social conflicts change over time. Let X_{it} denote the characteristics of the social conflict in period t that affect the decision of local authorities to apply violence against activists. The implementation of the MSM framework in the context of social conflicts follows the following (common) steps:

1. estimate the probability of the observed action (A_{it}) on the covariate ($\underline{X}_{it}$) and action history ($\underline{A}_{it-1}$). The sequential ignorability assumption requires in this step that the "correct" model of the action sequence be estimated. However, the relevant set of covariates and the functional form relating them to outcomes are unknown. To lend more credence to this assumption, I apply three different estimation methods for the action sequence model. First, I follow Blackwell (2013) and estimate a logit model with a preselected set of relevant covariates. Second, I rely on data-driven selection methods suggested by Montgomery and Olivella (2018) and, in a first

[28] The positivity assumption is closely related to the assumption of *common support* in the matching literature.

[29] Note that the data set is still heavily imbalanced; i.e., only in approximately 2.8% of all the 3-month intervals is police violence observed. This creates a challenge for learning algorithms. Appendix Section D.1.1 discusses how potential solutions can address this issue during the learning phase.

step, use a LASSO-logit model to determine which variables are most correlated with the decision to apply excessive force. Finally, I use gradient boosting machines (GBM) to accommodate potentially complex nonlinear functional forms and deep interactions (Montgomery and Olivella, 2018). I use 10-fold cross-validation to determine the optimal hyperparameter values for each of the two latter algorithms that minimize the out-of-sample logarithmic loss.

2. estimate the probability of the observed action (A_{it} on the action history ($\underline{A}_{it-1}$) and the baseline time period covariates (X_{i1}). Here, I again rely on the three estimation methods outlined in step 1.

3. calculate the "stabilized weight" for each social conflict as

$$SW_i = \prod_{t=1}^{T} \frac{\Pr\left(A_{it}|\underline{A}_{it-1}, X_{i1}\right)}{\Pr\left(A_{it}|\underline{A}_{it-1}, \underline{X}_{it}\right)}. \tag{4}$$

Note that, while the numerator could simply be assumed to be one, *stabilizing* the weights by the marginal probability of action conditional on past actions ($\underline{A}_{it-1}$) and predetermined baseline covariates X_{i1} (step 2) reduces the variability of the weights and increases efficiency.[30]

4. estimate the causal effect of the sequence of previous actions on the outcome of interest at time T using the estimated stabilized weights in a weighted (binomial) regression model. A common model choice for the MSM is to estimate a linear additive function of the form:

$$y_{iT} = \beta_0 + \beta_1 \left(\sum_{t=1}^{T} A_{it}\right) + \beta X_{iT} + \epsilon. \tag{5}$$

In the social conflict context, this model assumes that social conflicts that experienced the same number of total periods with police violence have similar potential

[30] As shown in Robins et al. (2000), this modeling choice of the numerator leaves the consistency of the MSM estimator intact. Following Montgomery and Olivella (2018), the hyperparameters for the LASSO-logit and GBM when I estimate the numerator are set to their optimal values found for the denominator in step 1.

outcomes. A simplifying assumption of this model is that violent suppression in the first six months of a conflict has the same effect as that in the last six months. Given the sparsity of police violence in the data, I also estimate a model specification assuming that social conflicts experiencing at least one incident of police violence have similar potential outcomes.

5. calculate the standard errors and confidence intervals by bootstrapping the entire estimation procedure, including the weights (Robins et al., 2000; Blackwell, 2013).[31]

More details on the algorithms used to estimate the IPTW and their performance and on the MSM model framework are provided in Appendix Section D.

3.2.3 Results

Stabilized Weights The critical step in the calculation of stabilized weights is to build the "correct" model for the action sequence $\overrightarrow{A_i} = A_{i1}, ..., A_{iT-1}$. This requires appropriate selection of covariates, interactions, and specific functional forms for the *standard* logit model. These requirements are gradually relaxed for LASSO-logit and GBM.[32] Table D.1 in the appendix provides an overview of the predictors used in each algorithm. Following Blackwell (2013), I restrict the estimation of IPTW to a sample with common support on baseline covariates due to empirical violations of the positivity assumption; i.e., stabilized weights for periods without any historically observed police violence across social conflicts are set to one.

The final distribution of stabilized weights by three-month intervals for each algorithm is presented in Figure 4.[33] As discussed in Cole and Hernán (2008), the mean of the estimated weights is required to equal one at each time period. Reassuringly, Panels B and C show that the average estimated weight for each 3-month interval is reasonably close to one, with the former exhibiting better-behaved weights. Moreover, the range of weights

[31] Note that social conflicts, not time periods, are resampled.

[32] Note that both LASSO-logit and GBM require preselection of all *potential* predictors while the standard logit model requires selection of the set of *relevant* predictors.

[33] Note that the social conflicts start at various times so that there are very few conflicts that continued over the course of more than 8 years (32 3-month intervals), but many lasted up to 3 years (12 3-month intervals).

is fairly narrow. For the standard generalized linear model (GLM), the weights are more variable, with extreme values pushing the mean of the weights away from one. Therefore, I follow the suggestion of Cole and Hernán (2008) and truncate the weights at the 97.5th and 2.5th percentiles to center the average weights around one. The distribution of the truncated weights is presented in Panel A.

MSM estimates Table 5 reports the MSM estimates and the bootstrapped 95% confidence intervals for the effect of police violence on the probability of a social conflict's ending in an official resolution agreement. The rows correspond to three different algorithms used to calculate the stabilized weights. Even columns assume that social conflicts that experienced *any* police violence have similar potential outcomes, while odd columns assume that conflicts with the same number of 3-month intervals with police violence have similar potential outcomes. The odd ratio estimates in column 1 provide some indication that the odds of an official resolution agreement are lower for conflicts with police violence. The results are similar if the MSM considers the total number of intervals with excessive force. However, the bootstrapped 95% confidence intervals include 1 and are wide in the case of the results with the XGBoost weights. A qualitatively similar pattern arises for the LPM. The marginal effect of police violence is estimated to be negative for all model specifications but remains insignificant, with the upper bound of the 95% confidence interval just above 0. As for the logit MSM, the effects are most precisely (imprecisely) estimated for the results using the LASSO-logit (XGBoost) weights.

In summary, the MSM estimates show a qualitatively robust pattern across model specifications: police violence decreases the probability of conflicts ending in "costly" resolution agreements. However, the noisily estimated effects should be interpreted only as suggestive evidence for the efficacy of excessive use of force.

4 Conclusion

This paper introduces a new data set on violent suppression of socioenvironmental advocacy against formal mining activity in Peru. Leveraging the spatial and temporal granularity of the data and changes in world mineral prices, I provide causal evidence on the positive relationship between local mineral rents and violent confrontations between protesters opposing local mining projects and the national police. Quantitatively, I estimate that a one-percentage-point increase relative to the mean in world prices of the main mineral mined in a municipality more than doubles the probability that I observe use of excessive force. Further, I show that this escalation in social conflicts is independent of the level of protester violence.

These baseline results are complemented with empirical evidence from municipality elections. Using a regression discontinuity design, I find that the narrow election of a pro-mining as opposed to an anti-mining candidate seems to increase the probability of excessive use of force against activists. Moreover, I find evidence of political capture of the judicial process. I find that the marginal election of a pro-mining mayor significantly decreases the probability of initial investigations into corruption during her term in office. However, when I consider only corruption cases with formal charges, the estimated effect points in the opposite direction, suggesting that investigations are misused as a political tool against anti-mining candidates.

Finally, I take a first step in the direction of providing causal estimates on the efficacy of violence in dispersing opposition. Taking advantage of the availability of information on the full timeline of each social conflict in the data set, I use a marginal structural model framework to estimate how the strategic use of excessive force affects the final outcome of the conflict. Formal resolution of social conflicts, which commonly involves financial compensation for environmental damages or use of land for local communities, is estimated to become less likely if violence is strategically applied over the course of a conflict.

This study's results contribute to the emerging literature on the political economy of human rights. The findings show that violence against agents of civil society constitutes an important negative externality of local mining activity even in stable democracies. Further, the present study highlights the potentially adverse effects of central government transfers of natural resource rents to local governments even if the use of those funds is regulated by law and free elections should ensure political accountability. This can help policymakers design redistribution schemes that internalize these externalities and align incentives of corporations, local authorities, and local community activists.

References

Agüero, J. M., Balcázar, C. F., Maldonado, S., and Ñopo, H. (2021). The value of redistribution: Natural resources and the formation of human capital under weak institutions. *Journal of Development Economics*, 148:102581.

Aragón, F. M. and Rud, J. P. (2013). Natural resources and local communities: Evidence from a peruvian gold mine. *American Economic Journal: Economic Policy*, 5(2):1–25.

Arce, M. (2014). *Resource extraction and protest in Peru*. University of Pittsburgh Press.

Arellano-Yanguas, J. (2011). Aggravating the resource curse: Decentralisation, mining and conflict in peru. *Journal of Development Studies*, 47(4):617–638.

Aresti, M. L. (2016). Mineral revenue sharing in peru. *Natural Resource Governance Institute*, pages 18–19.

Artiles, M., Kleine-Rueschkamp, L., and León-Ciliotta, G. (2021). Accountability, Political Capture, and Selection Into Politics: Evidence from Peruvian Municipalities. *Review of Economics and Statistics*, 103(2):397–411.

Asher, S. and Novosad, P. (2023). Rent-Seeking and criminal politicians: Evidence from mining booms. *Review of Economics and Statistics*, 105(1):20–39.

Baragwanath Vogel, K. (2021). *The effect of oil windfalls on political corruption: Evidence from Brazil*. PhD thesis, UC San Diego.

Bebbington, A., Humphreys Bebbington, D., Bury, J., Lingan, J., Muñoz, J. P., and Scurrah, M. (2008). Mining and social movements: Struggles over livelihood and rural territorial development in the andes. *World Development*, 36(12):2888–2905. Special Section: Social Movements and the Dynamics of Rural Development in Latin America (pp. 2874-2952).

Berman, N. and Couttenier, M. (2015). External shocks, internal shots: The geography of civil conflicts. *The Review of Economics and Statistics*, 97(4):758–776.

Berman, N., Couttenier, M., Rohner, D., and Thoenig, M. (2017). This mine is mine! How minerals fuel conflicts in Africa. *American Economic Review*, 107(6):1564–1610.

Berman, N., Couttenier, M., and Soubeyran, R. (2019). Fertile ground for conflict. *Journal of the European Economic Association*, 19(1):82–127.

Blackwell, M. (2013). A framework for dynamic causal inference in political science. *American Journal of Political Science*, 57(2):504–520.

Blackwell, M. (2014). A selection bias approach to sensitivity analysis for causal effects. *Political Analysis*, 22(2):169–182.

Bland, G. and Chirinos, L. A. (2014). Democratization through contention? regional and local governance conflict in peru. *Latin American Politics and Society*, 56(1):73–97.

Bodory, H., Huber, M., and Lafférs, L. (2022). Evaluating (weighted) dynamic treatment effects by double machine learning. *The Econometrics Journal*, 25(3):628–648.

Butt, N., Lambrick, F., Menton, M., and Renwick, A. (2019). The supply chain of violence. *Nature Sustainability*, 2(8):742–747.

Calonico, S., Cattaneo, M. D., and Titiunik, R. (2014). Robust nonparametric confidence intervals for regression-discontinuity designs. *Econometrica*, 82(6):2295–2326.

Canavire-Bacarreza, G. J., Martínez-Vázquez, J., and Sepulveda, C. F. (2012). Sub-national revenue mobilization in peru. *Andrew Young School of Policy Studies Research Paper Series*, (12-22):12–09.

Castellares, R., Fouché, M., et al. (2017). The determinants of social conflicts in mining production areas. Technical report.

Cattaneo, M. D., Idrobo, N., and Titiunik, R. (2020). *A practical introduction to regression discontinuity designs: Foundations*. Elements in Quantitative and Computational Methods for the Social Sciences. Cambridge University Press.

Cattaneo, M. D., Jansson, M., and Ma, X. (2018). Manipulation testing based on density discontinuity. *Stata Journal*, 18(1):234–261.

Clarke, D., Romano, J. P., and Wolf, M. (2020). The Romano–Wolf multiple-hypothesis correction in Stata. *Stata Journal*, 20(4):812–843.

Cole, S. R. and Hernán, M. A. (2008). Constructing inverse probability weights for marginal structural models. *American Journal of Epidemiology*, 168(6):656–664.

Colella, F., Lalive, R., Sakalli, S. O., and Thoenig, M. (2023). acreg: Arbitrary correlation regression. *Stata Journal*, 23(1):119–147.

Crabtree, J. (2014). Funding local government: Use (and abuse) of Peru's Canon system. *Bulletin of Latin American Research*, 33(4):452–467.

Davies, S., Pettersson, T., and Öberg, M. (2022). Organized violence 1989–2021 and drone warfare. *Journal of Peace Research*, 59(4):593–610.

Dube, O. and Vargas, J. F. (2013). Commodity price shocks and civil conflict: Evidence from colombia. *Review of Economic Studies*, 80(4 (285)):1384–1421.

Grasse, D. (2022). Oil crops and social conflict: Evidence from indonesia. *Journal of Conflict Resolution*, 66(7-8):1422–1448.

Harari, M. and Ferrara, E. L. (2018). Conflict, climate, and cells: A disaggregated analysis. *The Review of Economics and Statistics*, 100(4):594–608.

Harding, R., Prem, M., Ruiz, N. A., and Vargas, D. L. (2023). Buying a blind eye: Campaign donations, regulatory enforcement, and deforestation. *American Political Science Review*, page 1–19.

Haslam, P. A. and Ary Tanimoune, N. (2016). The determinants of social conflict in the latin american mining sector: New evidence with quantitative data. *World Development*, 78:401–419.

Heath, D., Ringgenberg, M. C., Samadi, M., and Werner, I. M. (2022). Reusing natural experiments. *Journal of Finance*, Forthcoming.

Hsiang, S. M., Burke, M., and Miguel, E. (2013). Quantifying the influence of climate on human conflict. *Science*, 341(6151):1235367.

Imai, K. and Ratkovic, M. (2015). Robust estimation of inverse probability weights for marginal structural models. *Journal of the American Statistical Association*, 110(511):1013–1023.

Knutsen, C. H., Kotsadam, A., Olsen, E. H., and Wig, T. (2017). Mining and local corruption in africa. *American Journal of Political Science*, 61(2):320–334.

Kreitmeir, D., Lane, N., and Raschky, P. (2020). The value of names - civil society, information, and governing multinationals on the global periphery. *Working Paper*.

Li, X., Zhou, Y., Zhao, M., and Zhao, X. (2020). A harmonized global nighttime light dataset 1992–2018. *Scientific data*, 7(1):168.

Loayza, N. and Rigolini, J. (2016). The local impact of mining on poverty and inequality: Evidence from the commodity boom in peru. *World Development*, 84:219–234.

Maldonado, S. (2011). Resource windfall and corruption: Evidence from peru. *Unpublished manuscript. UC Berkeley.*

Maldonado, S. (2017). The non-monotonic political effects of resource booms. *SSRN Working Paper 3153301.*

Maldonado, S. and Ardanaz, M. (2022). Natural resource windfalls and efficiency in local government expenditure: Evidence from peru. *Economics and Politics.*

Marshall, M. G., Gurr, T. R., Davenport, C., and Jaggers, K. (2002). Polity iv, 1800-1999: Comments on munck and verkuilen. *Comparative Political Studies*, 35(1):40–45.

McGuirk, E. and Burke, M. (2020). The economic origins of conflict in africa. *Journal of Political Economy*, 128(10):3940–3997.

Monfreda, C., Ramankutty, N., and Foley, J. A. (2008). Farming the planet: 2. Geographic distribution of crop areas, yields, physiological types, and net primary production in the year 2000. *Global Biogeochemical Cycles*, 22(1).

Montgomery, J. M. and Olivella, S. (2018). Tree-based models for political science data. *American Journal of Political Science*, 62(3):729–744.

Orihuela, J. C., Pérez, C. A., and Huaroto, C. (2019). Do fiscal windfalls increase mining conflicts? not always. *Extractive Industries and Society*, 6(2):313–318.

Pacheco Palacios, J. A., Yudith, V. E., and Cesar Augusto, O. R. (2022). El avance de la corrupción desde la perspectiva de la defensa jurídica del estado: Gobiernos regionales y locales. *Procuraduría Pública Especializada en Delitos de Corrupción.*

Robins, J., Hernán, M., and Brumback, B. (2000). Marginal structural models and causal inference in epidemiology. *Epidemiology*, 11(5):550—560.

Romano, J. P. and Wolf, M. (2005a). Exact and approximate stepdown methods for multiple hypothesis testing. *Journal of the American Statistical Association*, 100(469):94–108.

Romano, J. P. and Wolf, M. (2005b). Stepwise multiple testing as formalized data snooping. *Econometrica*, 73(4):1237–1282.

Romano, J. P. and Wolf, M. (2016). Efficient computation of adjusted p-values for resampling-based stepdown multiple testing. *Statistics & Probability Letters*, 113:38–40.

Sánchez De La Sierra, R. (2020). On the origins of the state: Stationary bandits and taxation in eastern congo. *Journal of Political Economy*, 128(1):32–74.

Schiavina, M., Freire, S., and MacManus, K. (2023). GHS-POP R2022A—GHS Population Grid Multitemporal (1975–2030). *European Commission, Joint Research Centre.*

Sexton, R. (2020). Unpacking the local resource curse: How externalities and governance shape social conflict. *Journal of Conflict Resolution*, 64(4):640–673.

Sundberg, R. and Melander, E. (2013). Introducing the ucdp georeferenced event dataset. *Journal of Peace Research*, 50(4):523–532.

5 Tables

Table 1: Descriptive Statistics: District Level (in %)

		Force used against protesters			Protester behavior	
		Pr(Arrests > 0)	Pr(Injuries > 0)	Pr(Casualties > 0)	Pr(Violence > 0)	Pr(Riots > 0)
All	N	355870	355870	355870	355870	355870
	Mean	0.013	0.038	0.008	0.008	0.012
	SD	1.161	1.955	0.871	0.918	1.073
Production	N	40850	40850	40850	40850	40850
	Mean	0.049	0.149	0.039	0.022	0.037
	SD	2.212	3.861	1.979	1.484	1.916
Concessions	N	53390	53390	53390	53390	53390
	Mean	0.036	0.079	0.011	0.024	0.030
	SD	1.886	2.804	1.060	1.560	1.731
None	N	261630	261630	261630	261630	261630
	Mean	0.003	0.013	0.002	0.003	0.004
	SD	0.587	1.123	0.437	0.553	0.618

Notes: All variables are presented in percent. Author's computation on basis of MIMEM and SNL Minings & Metals database.

Table 2: Social Conflict and Mineral Prices

	Force used against protesters			Protester behavior	
	Arrests	Injuries	Casualties	Violence	Riots
	(1)	(2)	(3)	(4)	(5)
$M\times$ ln(Price)	0.0004**	0.0019***	0.0007**	0.0002	0.0002
	(0.0002)	(0.0007)	(0.0003)	(0.0002)	(0.0002)
Dep. variable mean	0.0004	0.0011	0.0002	0.0002	0.0003
District $\times$ year FEs	✓	✓	✓	✓	✓
Observations	94241	94241	94241	94241	94241

Notes: M equals one for mining districts (production or concessions) and 0 otherwise. Ln(Price) denotes the natural logarithm of the main mineral price in month t. The main mineral in a district is determined by the *(i)* total production value and *(ii)* count of a concession's primary commodities. Heteroskedasticity- and autocorrelation-corrected standard errors accounting for spatial correlation of up to 500 km and unlimited serial correlation are obtained with the Stata module `acreg` (Colella et al., 2023). A linear decay in distance in the spatial correlation structure is assumed. * $p < 0.1$, ** $p < 0.05$, *** $p < 0.01$.

Table 3: Neighborhood Analysis

	Force used against protesters			Protester behavior	
	Arrests (1)	Injuries (2)	Casualties (3)	Violence (4)	Riots (5)
ln(Price)	0.0001	-0.0003	-0.0001	-0.0001	0.0000
	(0.0001)	(0.0003)	(0.0001)	(0.0002)	(0.0002)
$M\times$ ln(Price)	0.0010*	0.0022**	0.0007*	0.0005	0.0004
	(0.0006)	(0.0009)	(0.0004)	(0.0004)	(0.0005)
Dep. variable mean	0.00009	0.00028	0.00004	0.00008	0.0001
Neighbor $\times$ year FEs	✓	✓	✓	✓	✓
Month FEs	✓	✓	✓	✓	✓
Observations	1149880	1149880	1149880	1149880	1149880

Notes: M equals one for mining districts (production or concessions) and 0 otherwise. ln(Price) denotes the natural logarithm of the main mineral price in month t. The main mineral in a district is determined by the *(i)* total production value and *(ii)* count of a concession's primary commodities. Robust standard errors are clustered at the neighbor and month level. * $p < 0.1$, ** $p < 0.05$, *** $p < 0.01$.

Table 4: Summary Statistics – Social Conflict Level

	Any police violence					
	No = 0 (N = 248)		Yes = 1 (N = 67)			
	Mean	SD	Mean	SD	Diff. in Means	p-value
Resolved (%)	0.49	0.50	0.39	0.49	-0.10	0.13
Removed (%)	0.27	0.44	0.28	0.45	0.01	0.83
Censored (%)	0.24	0.43	0.33	0.47	0.09	0.16
3-month intervals w/ protests	0.94	1.19	2.39	4.35	1.45	0.01
3-month intervals w/ protester riots	0.03	0.17	0.09	0.29	0.06	0.10
Duration (3-month intervals)	9.56	10.01	16.28	16.30	6.72	0.00
Main mineral price (\$/kg)	9.03	13.45	12.45	14.95	3.42	0.09
Main crop price (\$/kg)	0.54	0.75	0.50	0.65	-0.04	0.65
Temperature (°C)	10.05	4.45	10.58	4.05	0.53	0.36
Rainfall (mm/month)	48.32	57.87	58.91	166.33	10.59	0.61
Canon minero$_0$ (\$1M)	2.03	5.17	3.51	8.62	1.48	0.18
Royalties$_0$ (\$1M)	0.42	1.61	0.59	1.33	0.17	0.38
Night light$_0$	2.09	3.74	2.51	3.00	0.43	0.33
Population density$_0$ (1/km^2)	56.29	175.69	45.93	85.82	-10.36	0.50
Indigenous population density$_0$ (1/km^2)	0.02	0.22	0.03	0.23	0.01	0.82
Road density$_0$ (1/km)	0.06	0.06	0.06	0.06	0.01	0.54
River density$_0$ (1/km)	0.26	0.05	0.26	0.05	0.00	0.48
Mean elevation$_0$ (km)	3.63	1.02	3.45	1.09	-0.18	0.23
Lake area$_0$ (%)	0.47	1.23	0.41	1.81	-0.06	0.81
Native community land$_0$ (%)	0.41	4.14	1.02	8.33	0.61	0.56
Indigenous land$_0$ (%)	0.00	0.00	0.00	0.00	0.00	0.69
Foreign Owner$_0$ (0/1)	0.48	0.50	0.57	0.50	0.08	0.23
Market Capitalization$_0$ (\$1B)	5.97	21.18	7.89	21.49	1.92	0.52
Leverage$_0$ (%)	2.86	8.22	4.32	10.13	1.46	0.28

Notes: The first four columns present basic statistics (mean and standard deviation) for social conflict characteristics across two "types" of conflicts: *(i)* social conflicts that never experienced police violence (column 1 and 2) and *(ii)* social conflicts that experienced *at least* one incident of police violence (column 3 and 4). Column 5 presents the difference in means between the two types of conflict for each conflict characteristic and column 6 presents the corresponding p-value for the null hypothesis of no significant difference.

Table 5: Effect of Police Violence on Likelihood of Official Resolution Agreement

	Logit		LPM	
	Binary	Sum	Binary	Sum
	(1)	(2)	(3)	(4)
GLM	0.527 [0.094,1.661]	0.571 [0.123,1.563]	-0.125 [-0.304,0.052]	-0.096 [-0.258,0.041]
LASSO	0.559 [0.118,1.579]	0.595 [0.137,1.519]	-0.112 [-0.282,0.050]	-0.090 [-0.243,0.036]
XGBoost	0.881 [0.100,3.306]	0.889 [0.105,3.275]	-0.069 [-0.277,0.132]	-0.066 [-0.269,0.125]

Notes: Bootstrapped 95% confidence intervals from 5,000 bootstrap samples are in brackets. Estimates are winsorized at the 0.5th and 99.5th percentiles. Row panels correspond to estimation model used for IPTW. Columns 1–2 and 3–4 present MSM estimates for logit and linear probability models, respectively. Even columns depict MSM estimates for a binary indicator of police violence during the course of the social conflict. Odd columns present MSM estimates for the total number of three-month intervals with police violence during the course of the social conflict.

6 Figures

Figure 1: Natural Resource Rents and Socioenvironmental Conflict

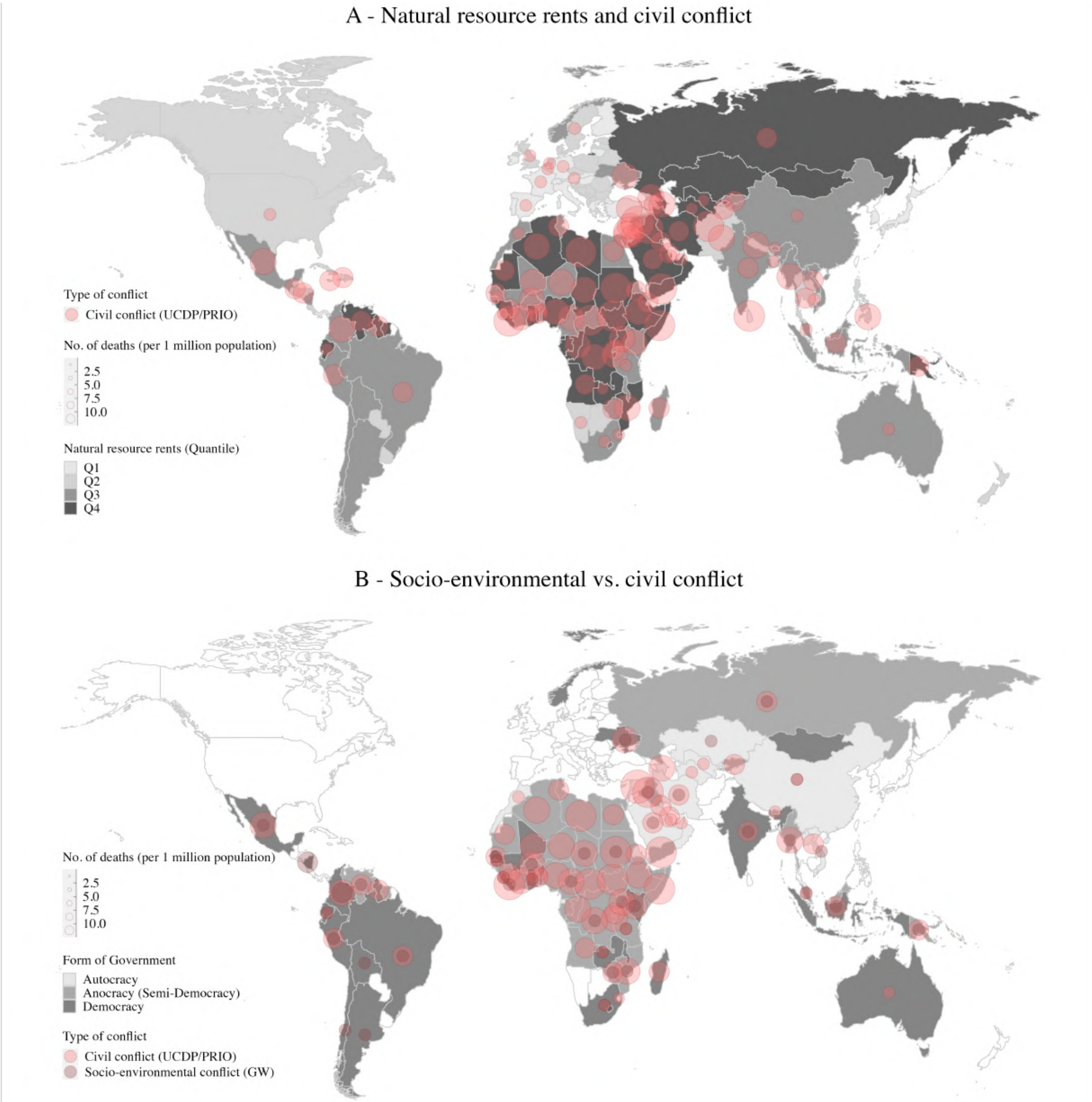

Notes: The sample period is from 2002 to 2019. Panel A presents the quantile distribution of average mineral rents (as percent of GDP) by country in sequentially darker shades of gray. Panel B is restricted to countries with above-median natural resource rents and displays their form of government. Countries are categorized on the basis of their *Polity2* score (Marshall et al., 2002) as follows: democracy ($5 < \text{Polity2} \leq 10$), anocracy ($-5 \geq \text{Polity2} \leq 5$), and autocracy ($-10 \geq \text{Polity2} \leq -5$). The "best" estimates of fatalities in civil conflicts registered in the *UCDP Georeferenced Event Dataset* (GED) Global version 22.1 (Sundberg and Melander, 2013; Davies et al., 2022) are presented as light-red-shaded point features. Panel B additionally displays in dark red the total number of killed "land and environmental defenders" as reported by *Global Witness*. Points are scaled in accordance with the inverse hyperbolic sine of the total number of deaths divided by the average population size in a country times one million. Data on population size and natural resource rents are taken from the *World Bank's World Development Indicators.*

Figure 2: Industrial Mining and Social Conflict

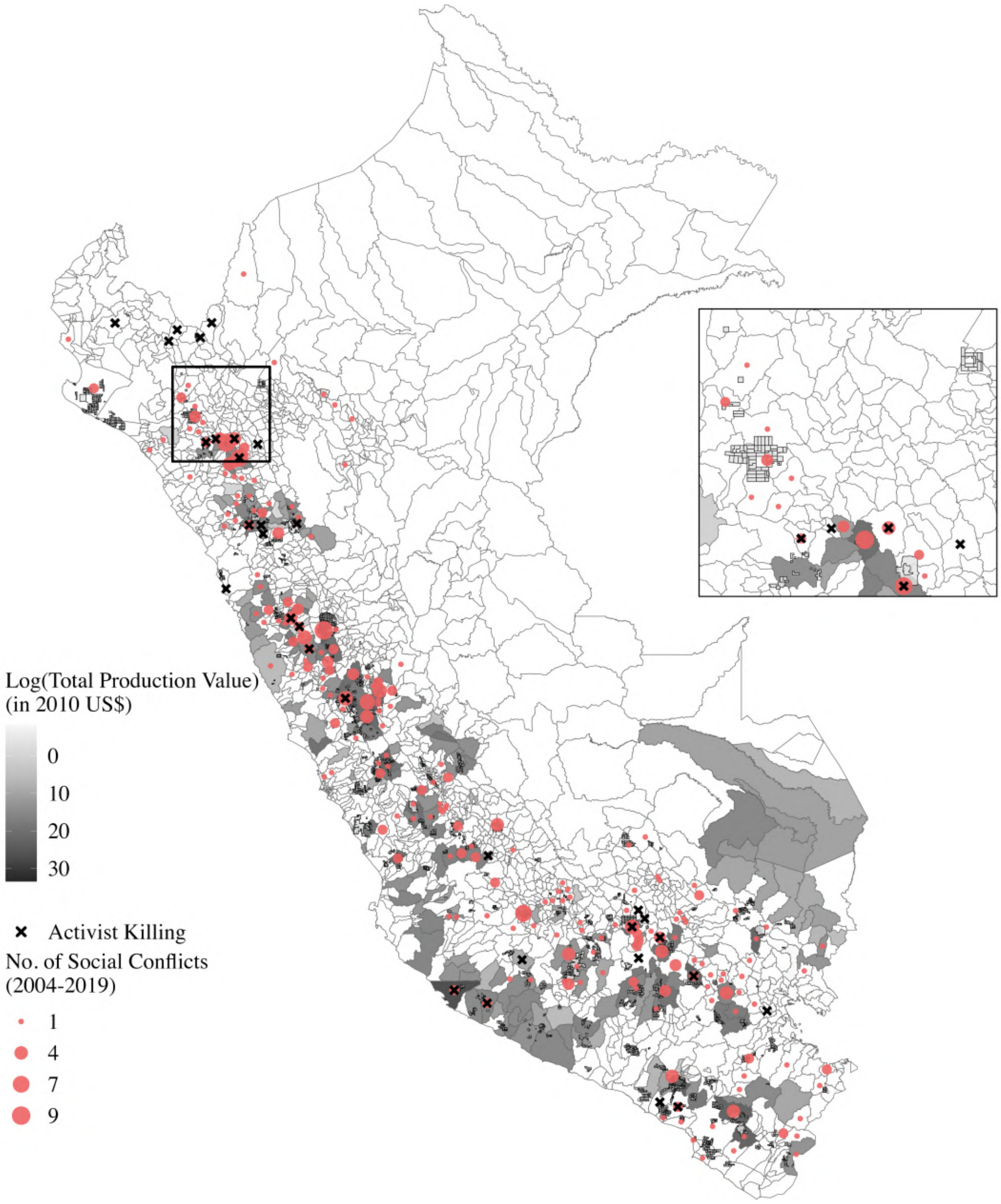

Notes: Boundary limits of districts—the third and lowest administrative level in Peru—are depicted. Mining concession areas are presented by the black-framed white areas.

Figure 3: Effect of Election of Pro-mining Politicians on Police Violence and Corruption

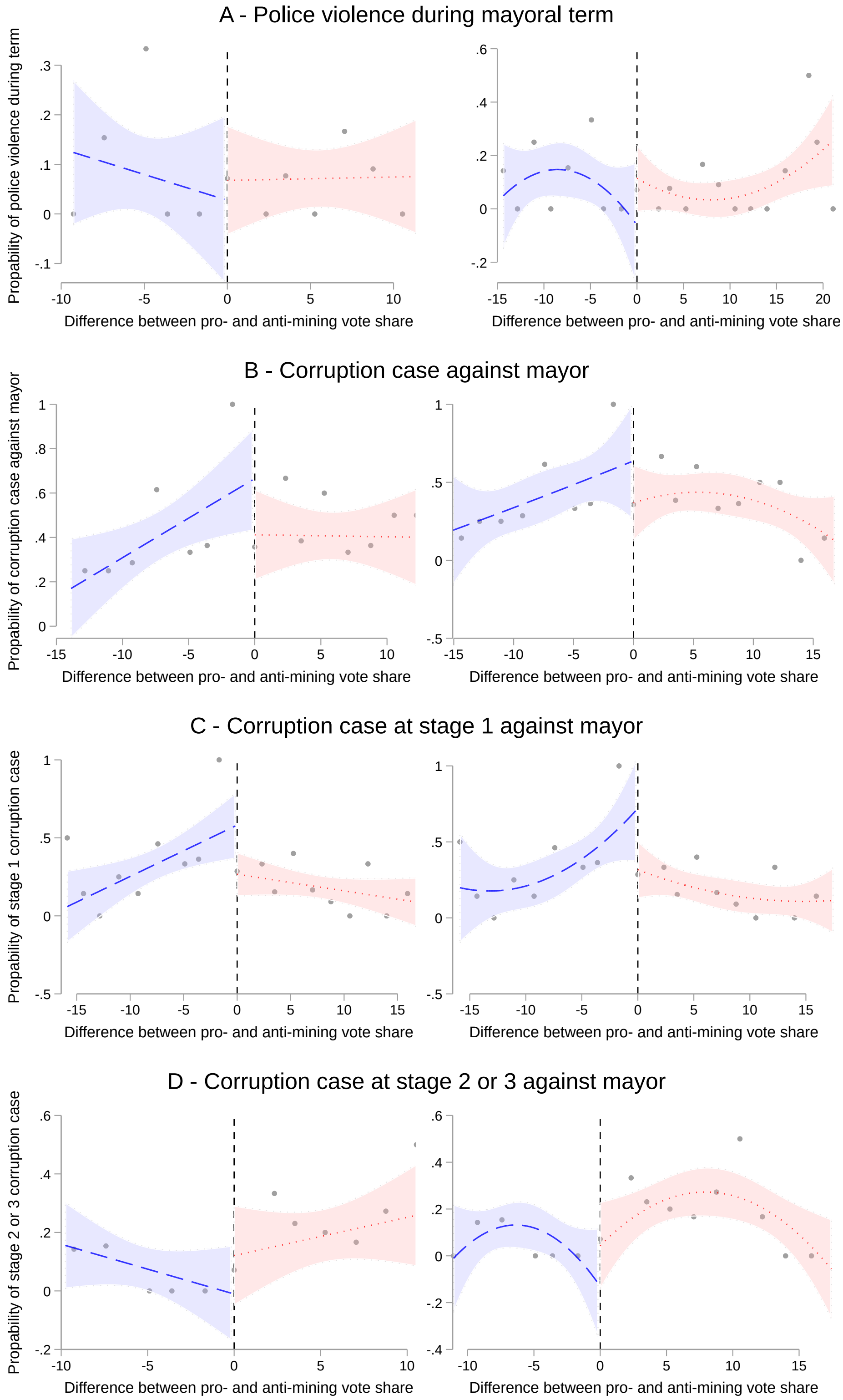

Notes: This figure presents a graphical approximation of the regression discontinuity design (Harding et al., 2023). Each panel presents the effects of (narrowly) electing a pro-mining politician over an anti-mining politician for a different outcome. Shaded areas denote 90% confidence intervals. The observations are shown within MSE-optimal bandwidths. Figures on the left use a linear polynomial approximation, while figures on the right use a quadratic approximation.

Figure 4: Stabilized Weights over the Course of Social Conflicts

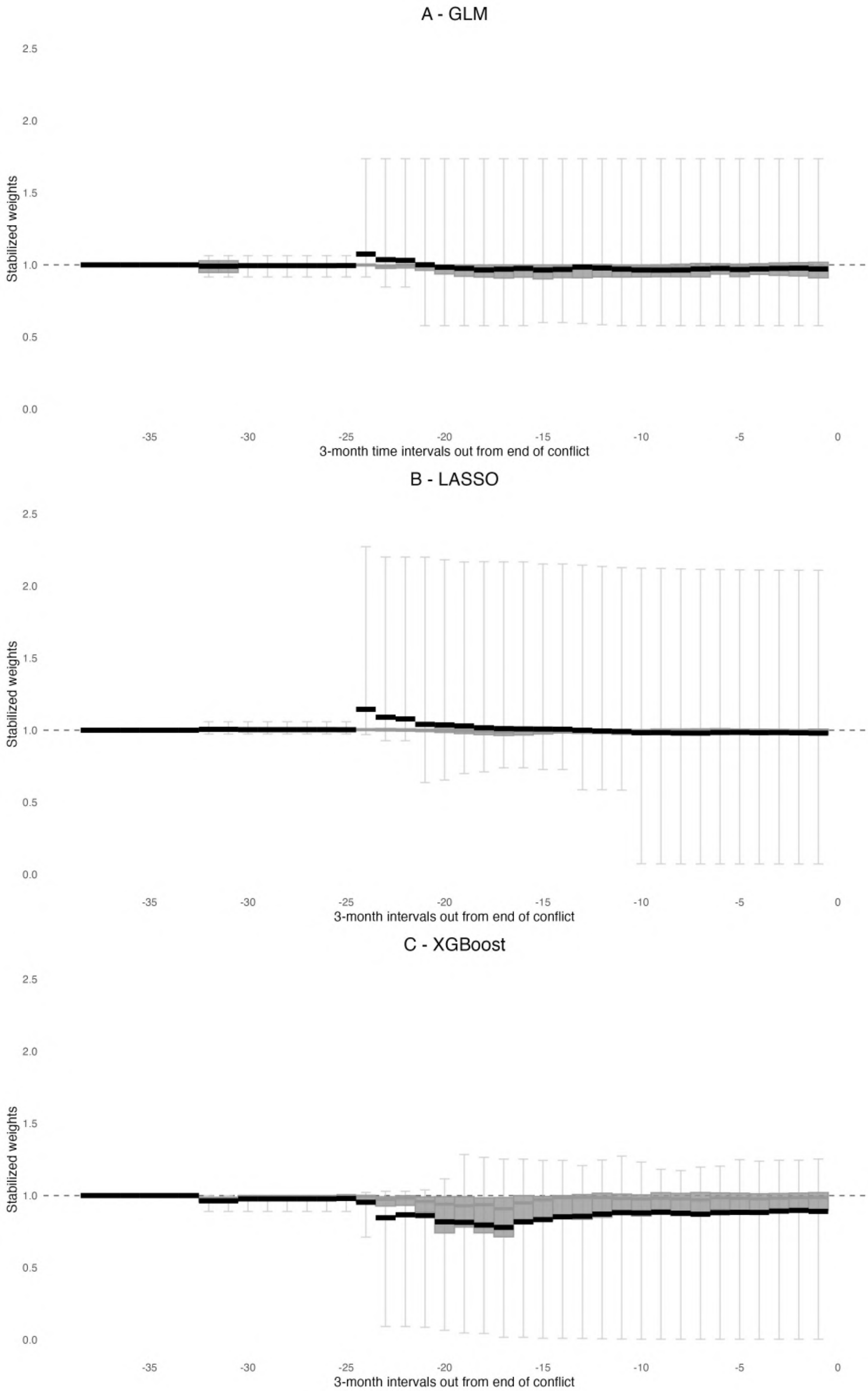

Notes: This figure presents the estimated stabilized weights over the course of social conflicts for three different estimators: (a) generalized additive models (GAM); (b) LASSO-logit models (LASSO); and (c) gradient-boosted machines (XGBoost). Black lines present three-month interval means across conflicts, gray rectangles denote interquartile ranges, and thin gray error bars present the range of the weights. Stabilized weights computed from GAM estimates are truncated at their 97.5th and 2.5th percentiles.

Supplementary Online Appendix

Table of Contents

A Data Appendix **1**

A.1 Social Conflicts 1

A.1.1 Social Conflict Data Set 1

A.1.2 Protest Data Set 2

A.1.3 Additional Figures 3

A.2 Government Plans 6

A.2.1 Classification of Government Plans 6

A.3 Mineral Prices 10

A.4 Variable Definitions 12

A.5 Summary Statistics 18

B Additional Results – Baseline Analysis **20**

B.1 Omitted Variables 20

B.2 Measurement 22

B.2.1 Main Mineral Price vs. Price Index 22

B.2.2 Outcomes 23

B.2.3 Producing Districts 25

B.3 Econometric Specification 26

B.3.1 Levels vs. Differences 26

B.4 Additional Robustness Checks 31

B.4.1 World Market Share 31

B.4.2 Spatial Kernel 32

B.4.3 Multiple Hypothesis Correction 33

C Democracy, Corruption, and Violence **35**

C.1 Manipulation Test 35

C.2 RDD Tables 36

D Dynamic Causal Inference **38**

D.1 Technical Appendix 38
D.1.1 Marginal Structural Models 38
D.1.2 LASSO 39
D.1.3 Gradient Boosting Machines 40
D.1.4 Covariates Included in Predictive Models of Police Violence . . 42
D.2 Model Performance 44
D.3 Directed Acyclic Graphs (DAGs) 47

A Data Appendix

A.1 Social Conflicts

A.1.1 Social Conflict Data Set

Peruvian Ombudsman Since April 2004, the Office of the Ombudsman (*Defensoría del Pueblo de Perú*) has published a monthly report on social conflicts in Peru. Each report follows a fairly consistent format.[34]

Figure A.1: Ombudsman Report Example Entry

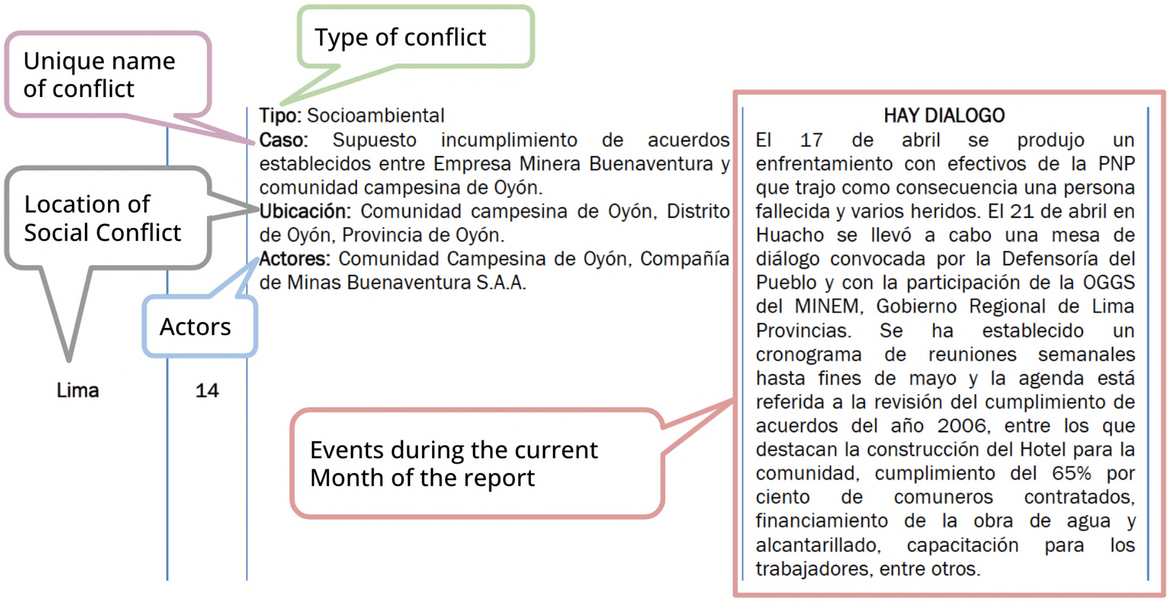

Source: Defensoría del Pueblo de Perú “Reporte de Conflictos Sociales Nº 86” (April 2014).

Mining Project Ownership I rely on Bureau van Dijk’s *Orbis* database to obtain corporate ownership information. *Orbis* reports shareholder history, allowing me to trace ownership of mining subsidiaries over the sample period from March 2004 to December 2019. I cross-validate this information against publicly available reports of corporations and authorities (e.g., SEC), the annual *USGS Mineral Yearbook* “Mineral Industry of Peru” reports and S&P’s SNL Metals and Mining dataset. The latter, moreover, provides information on the ownership of mining projects and concessions as well as their locations, allowing me to trace ownership even when no company name is noted in the reports.

Geoprecision Code The highest precision level, 1, is recorded as the default value of local social conflicts at the district level (ADMIN3). If the social conflict is noted to take place at the provincial (ADMIN2) or departmental (ADMIN1) level, the precision

[34] The ombudsman has updated the report’s outline over time, although key formats and information were preserved over the sample period. The report numbers for which the ombudsman made nonnegligible updates to the report outline are as follows: 3, 9, 11, 21, 35, 50, 72, and 90.

level is 2 or 3, respectively, and the province capital or department capital is used, unless previous or subsequent reports have information at a more granular level. In the latter case, the noted district- and/or province-level information in other reports is used.

A.1.2 Protest Data Set

Geoprecision Code If the report notes a particular town or district (ADMIN3), the highest precision level, 1, is recorded. If the source material notes the area around the mine or community, the geoprecision code is 2. The same code is applied if the mentioned location of the protest covers an area comprising multiple districts. If only the province (ADMIN2) is mentioned, the provincial capital is used, and the precision level is 3. If only the department and no other information is available, the departmental capital is used and noted with precision level 4.

A.1.3 Additional Figures

Figure A.2: Mineral Rents and Social Conflict (2004–2019)

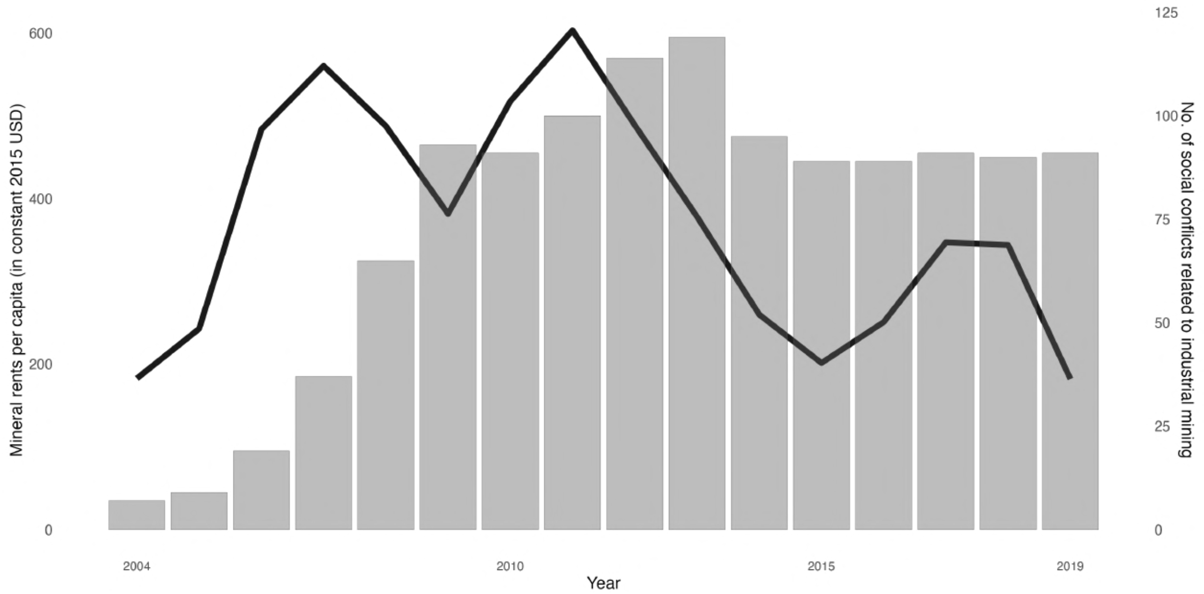

Notes: Mineral rents per capita (in constant 2015 USD) are computed from the *World Bank's World Development Indicators* and depicted by the black solid line. Grey bars display the number of social conflicts related to industrial mining and are calculated by the author on the basis of "*Conflictos sociales*" reports published by the Peruvian Office of the ombudsman (*Defensoria del Pueblo*).

Figure A.3: Social Conflict and Royalties

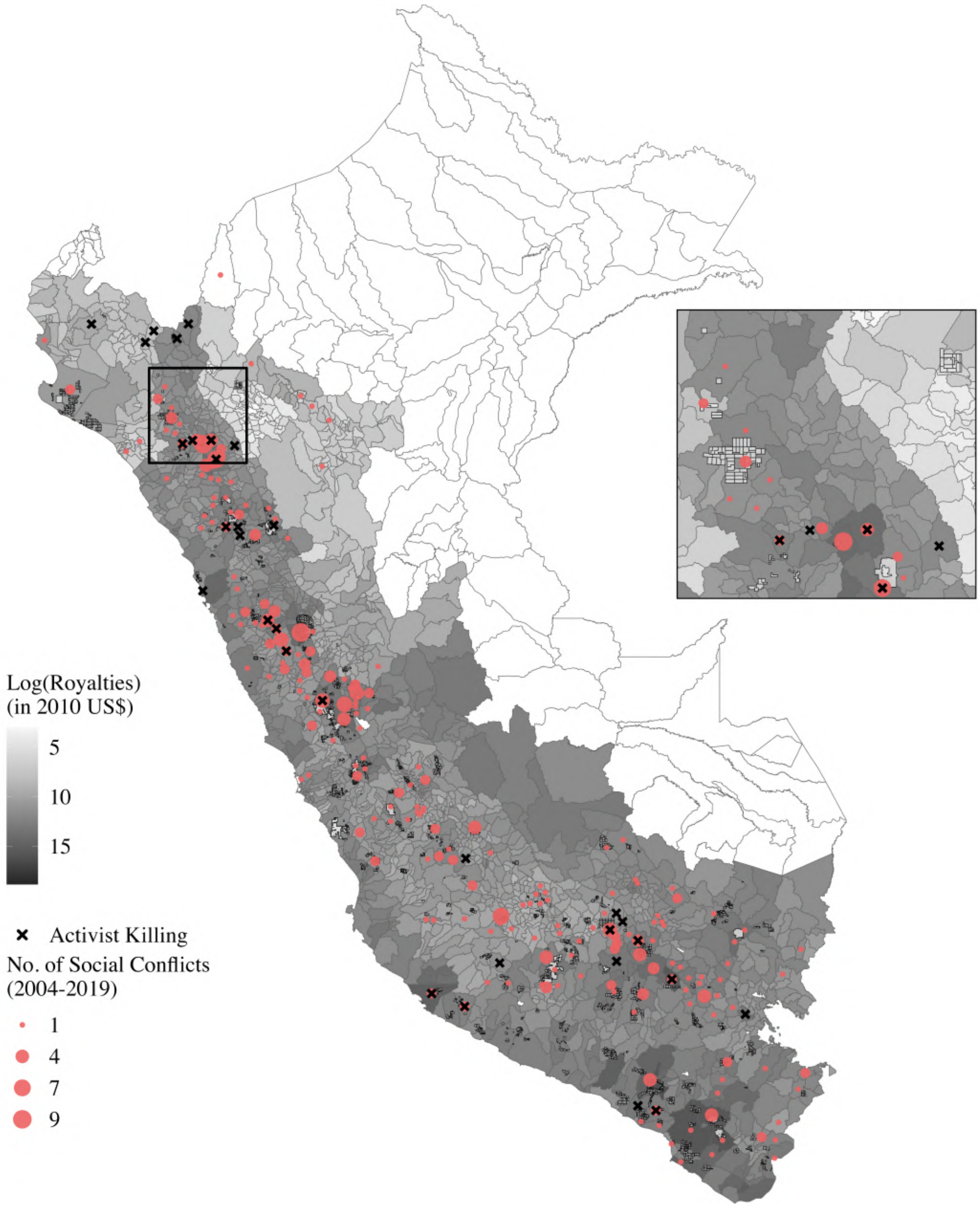

Notes: Boundary limits of districts–the third and lowest administrative level in Peru–are depicted. Mining concession areas are presented by the black framed white areas. Total transfers received by each district from mining royalties in real 2010 US dollars over the period from 2002-2019 are depicted.

Figure A.4: Social Conflict and Canon Minero

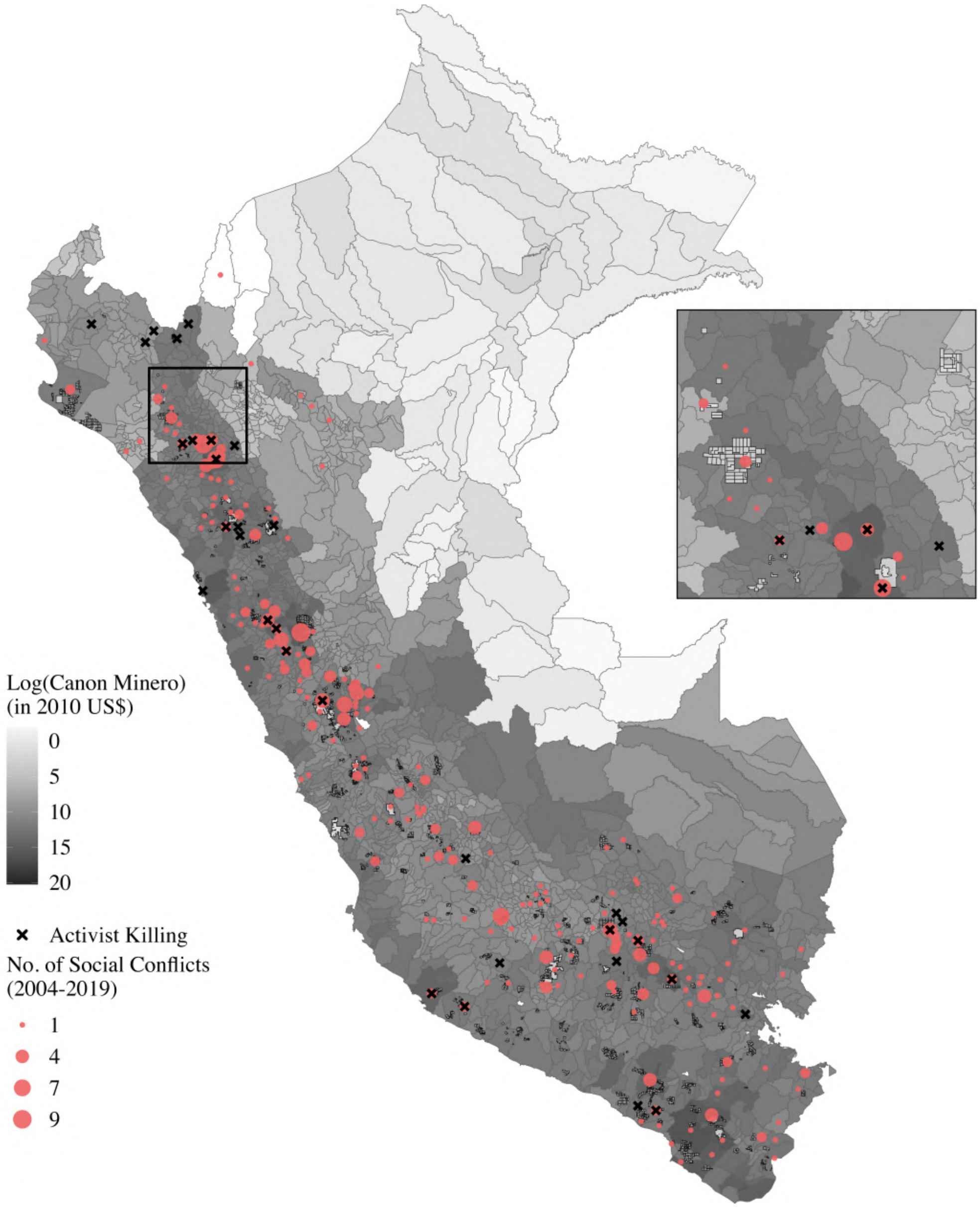

Notes: Boundary limits of districts–the third and lowest administrative level in Peru–are depicted. Mining concession areas are presented by the black framed white areas. Total transfers received by each district from *canon minero* in real 2010 US dollars over the period from 2002-2019 are depicted.

A.2 Government Plans

Figure A.5: Mayoral Candidate Government Plans

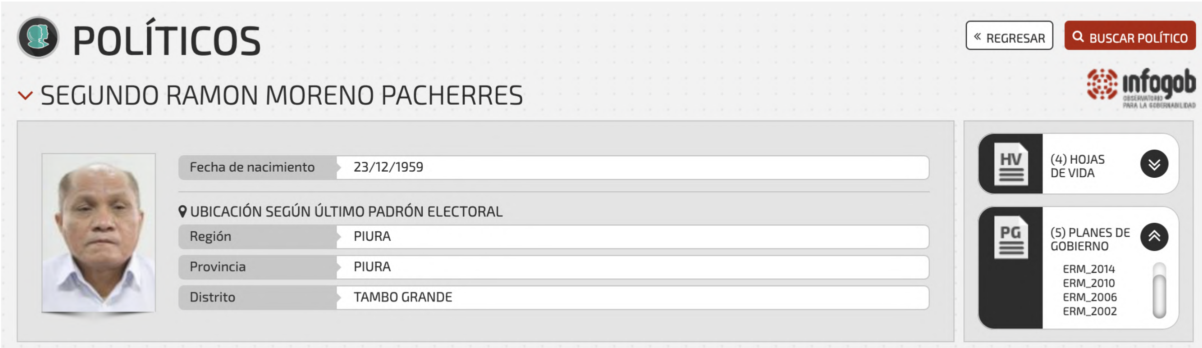

(a) Infogob profile of mayoral candidate

De esta manera el nuevo Municipio con sus autoridades ediles del período 2003 - 2006 , construirán un Municipio honesto, leal y capaz, poniendo a la persona como fin supremo de la sociedad y del Estado, un Municipio eficiente - productivo con una real vocación de servicio, que apueste por fortalecer la democracia y la descentralización en nuestra Patria, a través de la participación ciudadana y comunal..

Por esto y mucho más, presentamos a nuestro noble pueblo de Tambogrande y caseríos, nuestro Plan de Gobierno Municipal 2003 - 2006, bajo su lema "Desarrollo del Agro sin Minería".

(b) Government plan excerpt

Notes: The top panel presents the profile of a mayoral candidate in the *Infogob* database. The bottom panel displays an excerpt of the mayoral candidate's government plan for 2002. All available government plans can be accessed in the *planes de gobierno* window displayed at the bottom right corner in the top panel.
Source: https://infogob.jne.gob.pe/Politico/FichaPolitico/segundo-ramon-moreno-pacherres_historial-partidario_LqJgXVKnPC4=JV (last accessed 5 September 2023).

A.2.1 Classification of Government Plans

The classification procedure can be broadly summarized into these three (four) steps:

1. Preprocess government plans to obtain text corpus.
2. Filter government plans that (i) deal with mining and (ii) have relevant passages concerned with mining.
3. Ask GPT-4 to answer 5 questions based on the passages extracted in step 2 to determine the candidate's sentiment toward formal mining.

- If the answers are conflicting, feed text back to GPT-4 again with an adjusted prompt tailored toward resolving the conflict.

(4) If the classification procedure returns an error in any of the first three stages of the process, label the government reports manually.

Below, I elaborate on each of these steps.

Preprocessing I use the `python` libraries `pdfplumber` and `pytesseract` to extract text from pdf documents and scans and the `Linux` application `antiword` to process `.doc` Word documents. The text output is saved in a simple `.txt` file.

Filtering I use a semiautomatically generated keyword list to identify relevant mining terms in a text document. In particular, I use the pretrained Spanish word embeddings from Cardellino (2019) to obtain the top 50 most similar words (in cosine similiarity) to "*minera*". I clean the top 50 results of ambiguous (e.g., *minerales*) or irrelevant (e.g., *petrolera*) words and supplement the list with terms to identify mining corporations active in Peru (e.g., *bhp*). The final keyword list is: *carbonífera*, *barrick*, *yacimiento*, *copper*, *riotinto*, *bauxita*, *siderúrgico*, *minería*, *minero*, *mineros*, *aurífera*, *codelco*, *carbón*, *mineras*, *metalúrgicas*, *boliden*, *mina*, *glencore*, *siderúrgicas*, *siderurgia*, *mines*, *minas*, *mining*, *minera*, *spcc*, *plata*, *copper*, *zinc*, *minsur*, *shougang*, *silver*, *hudbay*, *marcobre*, *nexa*, *gold*, *shahuindo*, *coal*, *antamina*, *xstrata*, *newmont*, *bhp*, *doe*.
With the keyword list in hand, I use `spaCy` (Honnibal et al., 2020) to segment the text of each government plan document into sentences. I subsequently split each sentence into separate tokens (words) and compare each token against the keyword list.[35] I retain all sentences that include at least one keyword and a window of the 4 sentences before and after the sentence containing the keyword to retain contextual information. Finally, I combine all selected sentences to obtain a concise representation of the *relevant* passages of the original document.[36] Documents that do not contain any mining keywords are labeled "unknown."

GPT-4 The relevant passages for each government plan obtained in the previous step (denoted `.text_esp` below) are then used to send the following prompt to GPT-4:

```
[.text_esp]

From the text in Spanish above, answer the following questions.
Report results in a json array with a json object with three keys for each
    question: answer in English; reasoning in English; supporting quotes.
```

[35]I apply some simple preprocessing to trim excess whitespace and remove punctuation in each sentence.

[36]Note that I remove duplicates if the window of one sentence contains part of the window of another keyword sentence.

```
Provide reasoning up to 50 words.

* Does the text focus on the positive aspects of formal mining? Answer yes/
   no.
* Does the text suggest the promotion of formal mining activity? Answer yes
   /no.
* Does the text focus on the negative impacts of formal mining? Answer yes/
   no.
* Does the text suggest restrictions on formal mining activity? Answer yes/
   no.
* Is the text neutral towards formal mining? Answer yes/no.
```

The response from GPT-4 takes the following standardized form, as illustrated in the example output below:

```
[{
    "answer": "no",
    "reasoning": "The text does not focus on the positive aspects of formal
         mining.",
    "supporting_quotes": ""
},
{
    "answer": "no",
    "reasoning": "The text does not suggest the promotion of formal mining
        activity.",
    "supporting_quotes": ""
},
{
    "answer": "yes",
    "reasoning": "The text mentions the need for environmental impact
        studies and damage mitigation due to mining exploitation.",
    "supporting_quotes": "ejecutar estudios de impacto ambiental y
        mitigaci n de da os por la explotaci n de los recursos mineros de
         cuajone y quellaveco pr ximo a explotar."
},
{
    "answer": "yes",
    "reasoning": "The text suggests the implementation of an environmental
        management plan and the declaration of intangibility of certain
        areas.",
    "supporting_quotes": "plan de gesti n ambiental. declaraci n de
        intangibilidad de los arcos glaciares de arondaya."
},
{
    "answer": "no",
    "reasoning": "The text is not neutral towards formal mining as it
        highlights the need for environmental impact studies and damage
        mitigation.",
```

```
    "supporting_quotes": "ejecutar estudios de impacto ambiental y
        mitigaci n de da os por la explotaci n de los recursos mineros de
         cuajone y quellaveco pr ximo a explotar."
}]
```

The five questions are designed to allow classification of the government plan's sentiment toward mining—specifically, as *pro*, *anti*, or *neutral.* For instance, I classify a mayoral candidate as *pro*-mining if at least one of the first two questions is answered with "yes" (`Y`) by GPT-4 and the answers to questions three, four, and five are "no" (`N`). Below, I outline in detail how the answers translate to labels:

1. *pro*: `YYNNN`, `YYNYN`, `YNNNN`, `NYNNN`.
2. *anti*: `NNYYN`, `NYYYN`, `NNYNN`,`NNNYN`.
3. *neutral*: `NNNNY`, `NNNNN`.
4. *conflict*: otherwise

Government plans for which a logical conflict in the answers exists—e.g., if the focus is on both the benefits and negative impacts of formal mining (`YNYNN`)—the plans are fed back to GPT-4 with the following adjusted prompt:

```
[.text_esp]

From the text in Spanish above, answer the following question. Report
    results in a json array with a json object with three keys for each
    question: answer in English; reasoning in English; supporting quotes.
    Provide reasoning up to 50 words.
* Does the text focus on the benefits and promotion of formal mining or on
    the negative impact and restriction of formal mining? Answer benefits
    and promotion/negative impact/neither.
```

Errors If the classification procedure returns an error in any of the first three stages of the process, e.g., because the pdf document is protected, the government report is manually inspected and labeled by the principal investigator. Documents that cannot be classified due to the document's being password protected or containing only a blank page are treated as if missing.[37]

[37]In future iterations of the paper, a random sample of 10% of the GPT-4 responses will be drawn and cross-validated by human coders on *Amazon Mechanical Turk* or *Google Cloud's Vertex AI.*

A.3 Mineral Prices

Mineral price information at monthly (and yearly) frequency is retrieved from the *World Bank Commodity Price Data*.[38] The price development of each mineral over the period 2002–2020 is graphed in Figure A.6. At yearly frequency, I supplement the data set with digitized price information on minerals mined in Peru but not covered by the *World Bank* from the *USGS*'s "Mineral Commodity Summaries" or "Mineral Yearbooks."[39] Note that the *USGS* mineral prices do not reflect the world mineral price but the average price for the US. All mineral prices are converted to real USD with the MUV Index provided by the *World Bank* and uniformly expressed as $\$/kg$. A list of the minerals mined in Peru and priced at monthly and yearly frequency is provided below:

Monthly Mineral Prices:

- *World Bank*: Iron, Copper, Lead, Tin, Zinc, Gold, Silver.

Yearly Mineral Prices:

- *World Bank*: Iron, Copper, Lead, Tin, Zinc, Gold, Silver.
- *USGS*: Arsenic, Bismuth, Cadmium, Manganese, Molybdenum, Tungsten.

[38] For more details, see https://www.worldbank.org/en/research/commodity-markets#1.

[39] For more details, see https://www.usgs.gov/centers/national-minerals-information-center/commodity-statistics-and-information.

Figure A.6: Mineral Prices

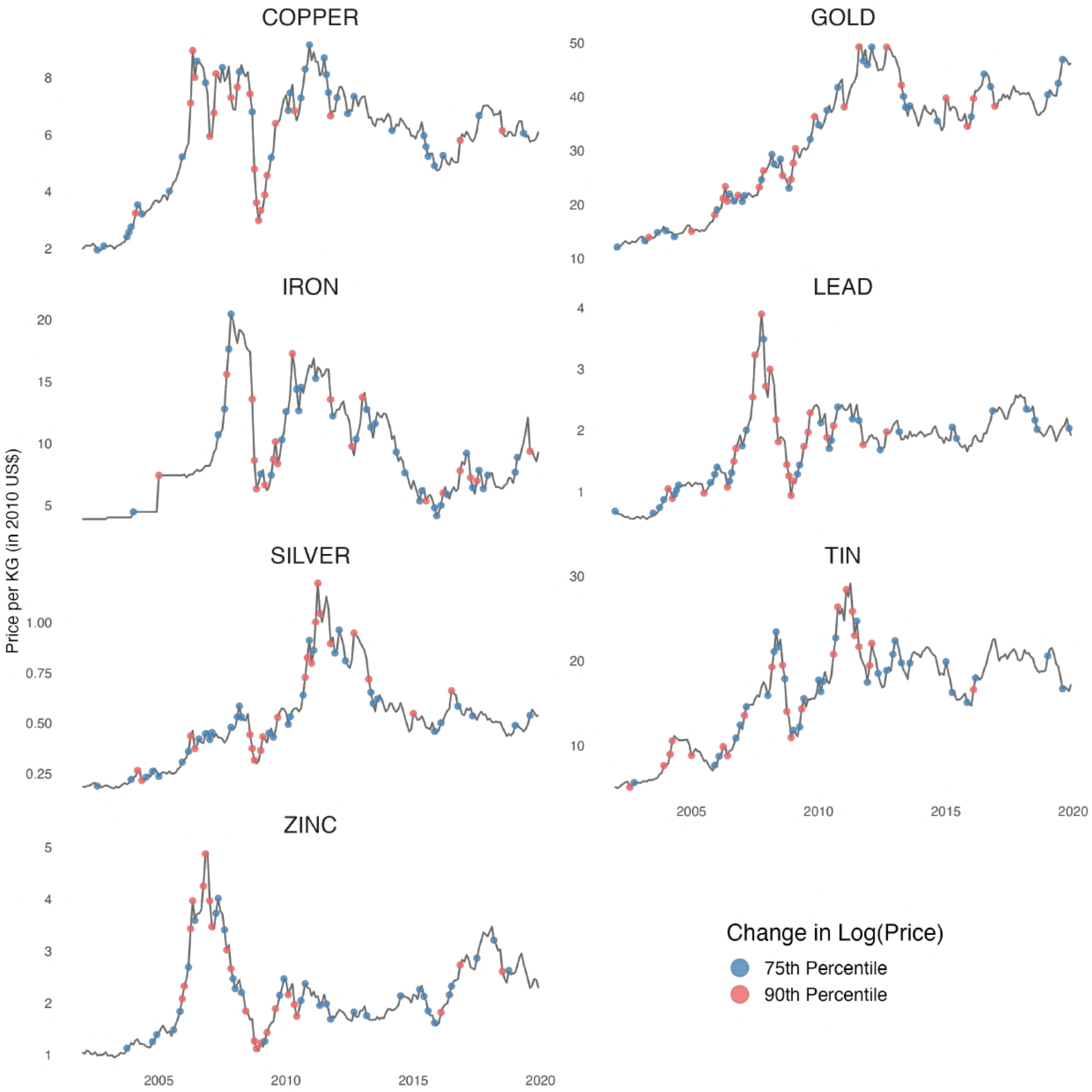

Notes: Prices for each mineral are expressed in real 2010 USD per kg for the period from January 2002 to December 2020.

A.4 Variable Definitions

Table A.1: Variable Definitions

Variable	Abbreviation	Description
Arrests	`arrests`	Dummy equaling 1 if at least one arrest of a protester was observed in district i in month t and 0 otherwise. Prefix `protest_` indicates that the district location of the event is used; `conflict_` indicates that the location(s) of the social conflict instead of the event location is (are) used. Suffix `_confirmed` indicates that only "confirmed" arrests are considered; `_wo_pr` indicates that months with protester riots are not considered and are coded as 0.
Injuries	`injuries`	Dummy equaling 1 if at least one injury of a protester was observed in district i in month t and 0 otherwise. Prefix `protest_` indicates that the district location of the event is used; `conflict_` indicates that the location(s) of the social conflict instead of the event location is used. Suffix `_confirmed` indicates that only "confirmed" injuries are considered; `_wo_pr` indicates that months with protester riots are not considered and are coded as 0.
Casualties	`casualties`	Dummy equaling 1 if at least one casualty among protesters was observed in district i in month t and 0 otherwise. Prefix `protest_` indicates that the district location of the event is used; `conflict_` indicates that the location(s) of the social conflict instead of the event location is used. Suffix `_wo_pr` indicates that months with protester riots are not considered and are coded as 0.
Killing	`killing`	Dummy equaling 1 if at least one casualty among activists was observed in district i in month t and 0 otherwise. This can include fatal violence during protests or assassinations.

Table A.1: Variable Definitions *(continued)*

Variable	Abbreviation	Description
Protester violence	`protester_violence`	Dummy equaling 1 if at least one incident of protester violence was observed in district i in month t and 0 otherwise. Prefix `protest_` indicates that the district location of the event is used; `conflict_` indicates that the location(s) of the social conflict instead of the event location is (are) used.
Protester riots	`protester_riots`	Dummy equaling 1 if at least one incident of violence or destruction of property by protesters was observed in district i in month t and 0 otherwise. Prefix `protest_` indicates that the district location of the event is used; `conflict_` indicates that the location(s) of the social conflict instead of the event location is (are) used.
Main mineral price	`price`	Main mineral price in month t for district i. The main mineral in a district is determined by *(i)* total production value or *(ii)* the primary commodity count of concessions (in nonproducing districts).
Price index	`avg_price`	Weighted price index in month t for district i. Weights are computed as each mineral's share of *(i)* total production value or *(ii)* the primary commodity count of concessions (in nonproducing districts).
Conflict resolution	`resolved`	Dummy equaling 1 in the last month where conflict c was active before an official resolution agreement between conflict parties was signed and equaling 0 otherwise.
Conflict removal	`removed`	Dummy equaling 1 in the last month where conflict c was active before the conflict was removed from the list of tracked conflicts by the Peruvian ombudsman due to inactivity and equaling 0 otherwise.

Table A.1: Variable Definitions *(continued)*

Variable	Abbreviation	Description
Conflict censoring	`censored`	Dummy equaling 1 in the last month before conflict c was right-censored either at the end of the sample period (December 2019) or because of unexplained removal from the list of conflicts tracked by the Peruvian ombudsman and equaling 0 otherwise.
Protest	`protest`	Dummy equaling 1 if at least one protest associated with social conflict c was observed in 3-month interval t and equaling 0 otherwise.
Protester riots	`protester_riots`	Dummy equaling 1 if at least one incident of violence or destruction of property by protesters associated with social conflict c was observed in 3-month interval t and equaling 0 otherwise.
Main mineral price	`avg_price`	Average of main mineral price in 3-month interval t across districts $i = 1, ..., N$ where social conflict c takes place. The main mineral in district i is determined by the *(i)* total production value or *(ii)* primary commodity count of concessions (in nonproducing districts).
Main crop price	`avg_crop_price`	Average of main crop prices in 3-month interval t across districts $i = 1, ..., N$ where social conflict c takes place. The main crop in district i is determined by the total production value of each crop with monthly price data coverage from the *World Bank*. Crop production for the year 2000 is obtained from *EarthStat* database (Monfreda et al., 2008).
Temper-ature	`avg_temp`	Average temperature in 3-month interval t across districts $i = 1, ..., N$ where social conflict c takes place. Data on temperature are obtained from the *CRU TS v4* database (Harris et al., 2020).
Rainfall	`avg_precip_sum`	Average precipitation in 3-month interval t across districts $i = 1, ..., N$ where social conflict c takes place. Data on monthly precipitation are obtained from the NOAA Global Precipitation Climatology Centre.

Table A.1: Variable Definitions *(continued)*

Variable	Abbreviation	Description
Duration	conflict_length	Length of conflict in 3-month intervals.
Canon minero	canon_minero	Total amount of *canon minero* obtained in a year by districts $i = 1, ..., N$ where social conflict c takes place.
Royalties	royalties	Total amount of royalties obtained in a year by districts $i = 1, ..., N$ where social conflict c takes place.
Nighttime Light	nl_mean	Average of nighttime lights across districts $i = 1, ..., N$ where social conflict c takes place. For consistency over time, the harmonized global nighttime light dataset from Li et al. (2020) is used.
Population density	pop_ghs_density	Number of citizens per km^2 across districts $i = 1, ..., N$ where social conflict c takes place. Data on population counts available at 5-year intervals are taken from the Global Human Settlement Layer Schiavina et al. (2023).
Indigenous population density	pop_indigena_density	Number of indigenous citizens per km^2 across districts $i = 1, ..., N$ where social conflict c takes place. Data on the number of indigenous citizens are taken from the *Mapeo territorial* of the *Instituto del Bien Común.*
Indigenous land (%)	perc_area_indigena	Ratio of indigenous land to total district area across districts $i = 1, ..., N$ where social conflict c takes place. Data on indigenous areas are taken from the *Mapeo territorial* of the *Instituto del Bien Común.*
Native communities land (%)	perc_area_nativa	Ratio of land inhabited by native communities to total district area across districts $i = 1, ..., N$ where social conflict c takes place. Data on native community areas are taken from the *Mapeo territorial* of the *Instituto del Bien Común.*

Table A.1: Variable Definitions *(continued)*

Variable	Abbreviation	Description
Road density	road_density	Road length (in km) relative to district area (km^2) averaged across districts $i = 1, ..., N$ where social conflict c takes place. Data on the Peruvian road network are obtained from the *Ministerio de Transportes y Comunicaciones*.
Lake area (%)	perc_lake	Ratio of land covered by lakes to total area across districts $i = 1, ..., N$ where social conflict c takes place. Data on lake sizes are obtained from the *HydroSheds* database.
River density	river_density	Length of rivers (in km) relative to district area (km^2) across districts $i = 1, ..., N$ where social conflict c takes place. Data on waterways are obtained from the *HydroSheds* database.
Elevation	elev_mean	Average elevation across districts $i = 1, ..., N$ where social conflict c takes place. Elevation data are obtained from *SRTM* v4 dataset.
HQ country of majority owner(s)	MajorityOwnerLoc	Categorical variable that can take 3 mutually exclusive values: (i) "foreign" if (at least one of) the majority owner(s) of the mine/project associated with conflict c is (are) headquartered outside of Peru, (ii) "local" if the majority owner(s) is (are) Peruvian, and (iii) "N/A" if no information on the location of the owner(s) is available. Historical ownership shares are obtained from Bureau van Dijk's *Orbis* database and cross-validated with annual reports if available. Location information is obtained from *Orbis* and S&P's *Compustat* database.
Market capitalization of majority owner(s)	mkvalt	Market value (US$) of the majority owner(s) of mine/project associated with conflict c. The average market value is used if there is more than one publicly traded majority owner. Data on market capitalization are obtained from S&P's *Compustat* database.

Table A.1: Variable Definitions *(continued)*

Variable	Abbreviation	Description
Leverage of majority owner(s)	`leverage`	Ratio of total debt to total assets of the majority owner(s) of mine/project associated with conflict c. The average ratio is used if there is more than one publicly traded majority owner. Data on total debt and assets are obtained from S&P's *Compustat* database.
Police violence	`police_violence`	Dummy equaling 1 if at least one incident of violence (fatal or nonfatal) against protesters associated with social conflict c was observed in 3-month interval t and equaling 0 otherwise
Political competition	`polcomp`	Political competition is calculated as the inverse of the sum of squared vote shares of each candidate within an electoral race (Artiles et al., 2021).
Win margin	`x`	Margin in votes between pro-mining and anti-mining candidate; > 0 if the pro-mining candidate wins the election, and < 0 if the anti-mining candidate wins the election.

A.5 Summary Statistics

Table A.2: District Government Revenues from Royalties and *Canon Minero* (2002–2019)

		N	Mean	Median	SD	Min	Max
All	*Canon Minero* (in 2010 USD)	1873	6,213,556	941,625	22,433,363	0	535,857,094
	Royalties (in 2010 USD)	1873	1,278,833	236,485	5,005,074	0	77,952,062
Production	*Canon Minero* (in 2010 USD)	215	18,701,791	4,811,426	48,552,674	4,275	535,857,094
	Royalties (in 2010 USD)	215	4,580,338	1,153,231	11,737,776	0	77,952,062
Concessions	*Canon Minero* (in 2010 USD)	281	10,140,780	2,077,637	28,146,551	599	314,122,841
	Royalties (in 2010 USD)	281	1,912,803	451,413	5,707,105	472	72,085,687
None	*Canon Minero* (in 2010 USD)	1377	3,462,270	524,076	11,033,366	0	198,282,741
	Royalties (in 2010 USD)	1377	633,976	150,223	1,955,571	0	39,808,289

Notes: Author's computation on the basis of data from the *Ministerio de Economía y Finanzas* (MNF).

Table A.3: World Production Shares by Commodity

	(1) Copper	(2) Gold	(3) Iron	(4) Lead	(5) Silver	(6) Tin	(7) Zinc
Panel A: Peru (Total)							
2002	6.2	5.4	0.3	10.0	13.4	18.5	13.2
2003	6.1	6.6	0.3	10.4	14.8	18.4	13.9
2004	7.1	7.1	0.3	9.7	15.5	15.9	12.5
2005	6.7	8.4	0.3	9.8	16.5	14.5	12.2
2006	6.9	8.3	0.3	9.0	17.2	12.6	12.0
2007	7.7	7.1	0.2	8.7	16.8	12.2	13.2
2008	8.2	8.0	0.2	9.0	17.3	13.0	13.8
2009	8.0	7.4	0.2	7.8	17.7	14.4	13.5
2010	7.9	6.4	0.2	6.3	15.8	12.8	12.2
2011	7.7	6.2	0.2	4.9	14.6	11.8	9.8
2012	7.7	6.0	0.2	4.8	13.6	10.9	9.5
2013	7.5	5.4	0.2	4.8	14.1	8.1	10.1
2014	7.5	4.7	0.2	5.7	14.1	8.1	9.9
2015	8.9	4.7	0.3	6.4	4.7	6.7	11.1
2016	11.7	4.9	0.6	6.7	17.0	6.5	10.6
2017	12.2	4.7	0.6	6.7	16.0	5.7	11.8
2018	12.0	4.3	0.6	6.3	15.5	5.8	11.8
2019	12.1	3.9	0.7	6.5	14.6	6.7	11.0
Panel B: District (Max)							
2002	2.5	1.7	0.3	3.9	2.0	18.5	3.3
2003	1.9	2.0	0.3	3.7	1.9	18.4	4.0
2004	2.6	1.9	0.3	3.2	1.9	15.9	3.0
2005	2.6	3.4	0.3	3.3	2.0	14.5	2.8
2006	2.6	3.3	0.3	1.4	1.6	12.6	2.0
2007	2.2	2.0	0.2	1.7	1.7	12.2	3.1
2008	2.3	2.5	0.2	1.7	2.0	13.0	3.5
2009	2.2	2.6	0.2	1.1	2.3	14.4	4.6
2010	2.1	1.8	0.2	0.7	2.1	12.8	3.6
2011	2.2	1.4	0.2	0.6	1.6	11.8	2.1
2012	2.7	1.2	0.2	0.6	1.6	10.9	2.0
2013	2.5	0.7	0.2	0.7	2.0	8.1	2.4
2014	2.0	0.7	0.2	0.7	1.6	8.1	2.0
2015	2.2	0.9	0.3	0.7	0.7	6.7	2.3
2016	2.6	0.6	0.6	0.7	2.5	6.5	2.1
2017	2.5	0.5	0.6	0.7	2.3	5.7	3.5
2018	2.4	0.5	0.6	0.6	2.0	5.8	3.8
2019	2.3	0.5	0.7	0.6	1.8	6.7	2.8

Notes: Data on world production of minerals is obtained from the USGS *Mineral Commodity Summaries*. Production data by mineral for Peru at the national and district levels are obtained from USGS and MINEM.

B Additional Results – Baseline Analysis

B.1 Omitted Variables

Table B.1: Neighborhood Analysis – 10 Nearest Neighbors

	Force used against protesters			Protester behavior	
	Arrests	Injuries	Casualties	Violence	Riots
	(1)	(2)	(3)	(4)	(5)
ln(Price)	0.0000	-0.0005	-0.0002**	-0.0003	-0.0004
	(0.0001)	(0.0003)	(0.0001)	(0.0002)	(0.0002)
$M\times$ ln(Price)	0.0011**	0.0022**	0.0007*	0.0005	0.0005
	(0.0005)	(0.0009)	(0.0004)	(0.0004)	(0.0005)
Neighbor × year FEs	✓	✓	✓	✓	✓
Month FEs	✓	✓	✓	✓	✓
Observations	564110	564110	564110	564110	564110

Notes: M equals one for mining districts (production or concessions) and 0 otherwise. ln(Price) denotes the natural logarithm of the main mineral price in month t. The main mineral in a district is determined by the *(i)* total production value and *(ii)* count of a concession's primary commodities. Robust standard errors are clustered at the neighbor and month level. * $p < 0.1$, ** $p < 0.05$, *** $p < 0.01$.

Table B.2: Additional Time-Varying Controls

	Force used against protesters												Protester behavior							
	Arrests				Injuries				Casualties				Violence				Riots			
	(1)	(2)	(3)	(4)	(5)	(6)	(7)	(8)	(9)	(10)	(11)	(12)	(13)	(14)	(15)	(16)	(17)	(18)	(19)	(20)
$M\times$ ln(Price)	0.0004*	0.0004**	0.0003	0.0003	0.0019**	0.0019***	0.0018**	0.0018**	0.0006**	0.0007**	0.0006**	0.0006**	0.0002	0.0002	0.0002	0.0002	0.0002	0.0002	0.0002	0.0002
	(0.0002)	(0.0002)	(0.0002)	(0.0002)	(0.0008)	(0.0007)	(0.0007)	(0.0007)	(0.0003)	(0.0003)	(0.0003)	(0.0003)	(0.0002)	(0.0002)	(0.0002)	(0.0002)	(0.0002)	(0.0002)	(0.0002)	(0.0002)
Ln(Crop price)	-0.0001			0.0000	0.0001			0.0002	0.0003			0.0004	-0.0001			0.0000	-0.0001			0.0000
	(0.0004)			(0.0004)	(0.0009)			(0.0009)	(0.0004)			(0.0004)	(0.0003)			(0.0003)	(0.0003)			(0.0003)
Ln(Temperature)		-0.0002		0.0001		-0.0002		0.0003		0.0000		0.0001		-0.0002		0.0000		-0.0004		0.0000
		(0.0003)		(0.0003)		(0.0005)		(0.0007)		(0.0003)		(0.0004)		(0.0002)		(0.0003)		(0.0003)		(0.0004)
Ln(Precipitation)			0.0000	0.0000			-0.0001	-0.0001			0.0000	0.0000			-0.0001	-0.0001			-0.0001*	-0.0001
			(0.0000)	(0.0000)			(0.0001)	(0.0001)			(0.0000)	(0.0000)			(0.0000)	(0.0000)			(0.0000)	(0.0001)
District $\times$ year FEs	✓	✓	✓	✓	✓	✓	✓	✓	✓	✓	✓	✓	✓	✓	✓	✓	✓	✓	✓	✓
Observations	94240	94240	88065	88065	94240	94240	88065	88065	94240	94240	88065	88065	94240	94240	88065	88065	94240	94240	88065	88065

Notes: M equals one for mining districts (production or concessions) and 0 otherwise. ln(Price) denotes the natural logarithm of the main mineral price in month t. The main mineral in a district is determined by the *(i)* total production value and *(ii)* count of a concession's primary commodities. Heteroskedasticity- and autocorrelation-corrected standard errors accounting for spatial correlation of up to 500 km and unlimited serial correlation are obtained with the Stata module `acreg` (Colella et al., 2023). A linear decay in distance in the spatial correlation structure is assumed. * $p < 0.1$, ** $p < 0.05$, *** $p < 0.01$.

B.2 Measurement

B.2.1 Main Mineral Price vs. Price Index

Table B.3: Price Index vs. Main Mineral Price

	Force used against protesters			Protester behavior	
	Arrests	Injuries	Casualties	Violence	Riots
	(1)	(2)	(3)	(4)	(5)
$M\times$ ln(Price index)	0.0004*	0.0013**	0.0005**	0.0003	0.0002
	(0.0002)	(0.0005)	(0.0002)	(0.0002)	(0.0002)
District × year FEs	✓	✓	✓	✓	✓
Observations	94240	94240	94240	94240	94240

Notes: M equals one for mining districts (production or concessions) and 0 otherwise. Ln(Price index) denotes the natural logarithm of the weighted price index in month t. Weights are computed as each mineral's share of the *(i)* total production value or *(ii)* count of a concession's primary commodities. Heteroskedasticity- and autocorrelation-corrected standard errors accounting for spatial correlation of up to 500 km and unlimited serial correlation are obtained with the Stata module `acreg` (Colella et al., 2023). A linear decay in distance in the spatial correlation structure is assumed. * $p < 0.1$, ** $p < 0.05$, *** $p < 0.01$.

B.2.2 Outcomes

Table B.4: Alternative Coding of Outcomes

		Excl. "unconfirmed" events		Excl. months with protester riots		
	Killing	Arrests	Injuries	Arrests	Injuries	Casualties
	(1)	(2)	(3)	(4)	(5)	(6)
$M\times$ ln(Price)	0.0003	0.0002	0.0011**	0.0003*	0.0017**	0.0006**
	(0.0002)	(0.0001)	(0.0005)	(0.0002)	(0.0007)	(0.0002)
District × year FEs	✓	✓	✓	✓	✓	✓
Observations	95232	94223	94185	94209	94209	94209

Notes:
M equals one for mining districts (production or concessions) and 0 otherwise. Ln(Price) denotes the natural logarithm of the main mineral price in month t. The main mineral in a district is determined by the *(i)* total production value and *(ii)* count of a concession's primary commodities. Heteroskedasticity- and autocorrelation-corrected standard errors accounting for spatial correlation of up to 500 km and unlimited serial correlation are obtained with the Stata module `acreg` (Colella et al., 2023). A linear decay in distance in the spatial correlation structure is assumed. * $p < 0.1$, ** $p < 0.05$, *** $p < 0.01$.

Table B.5: Social Conflict vs. Event Location

	Force used against protesters			Protester behavior	
	Arrests	Injuries	Casualties	Violence	Riots
	(1)	(2)	(3)	(4)	(5)
$M\times$ ln(Price)	0.0004	0.0010**	0.0003	0.0002	0.0002
	(0.0003)	(0.0005)	(0.0002)	(0.0002)	(0.0002)
District $\times$ year FEs	✓	✓	✓	✓	✓
Observations	94240	94240	94240	94240	94240

Notes: M equals one for mining districts (production or concessions) and 0 otherwise. Ln(Price) denotes the natural logarithm of the main mineral price in month t. The main mineral in a district is determined by the *(i)* total production value and *(ii)* count of a concession's primary commodities. Heteroskedasticity- and autocorrelation-corrected standard errors accounting for spatial correlation of up to 500 km and unlimited serial correlation are obtained with the Stata module `acreg` (Colella et al., 2023). A linear decay in distance in the spatial correlation structure is assumed. * $p < 0.1$, ** $p < 0.05$, *** $p < 0.01$.

B.2.3 Producing Districts

Table B.6: Producing Districts

	Force used against protesters			Protester behavior	
	Arrests	Injuries	Casualties	Violence	Riots
	(1)	(2)	(3)	(4)	(5)
$M\times$ ln(Price)	0.0010*	0.0013	0.0006	0.0003	0.0001
	(0.0005)	(0.0009)	(0.0004)	(0.0002)	(0.0003)
District $\times$ year FEs	✓	✓	✓	✓	✓
Observations	40850	40850	40850	40850	40850

Notes: M equals one for mining districts (production only) and 0 otherwise. Ln(Price) denotes the change in the logarithm of the main mineral price from month $t-1$ to t. The main mineral in a district is determined exclusively by the total production value. Heteroskedasticity- and autocorrelation-corrected standard errors accounting for spatial correlation of up to 500 km and unlimited serial correlation are obtained with the Stata module `acreg` (Colella et al., 2023). A linear decay in distance in the spatial correlation structure is assumed. * $p < 0.1$, ** $p < 0.05$, *** $p < 0.01$.

B.3 Econometric Specification

B.3.1 Levels vs. Differences

Figure B.1: Unit Root Test

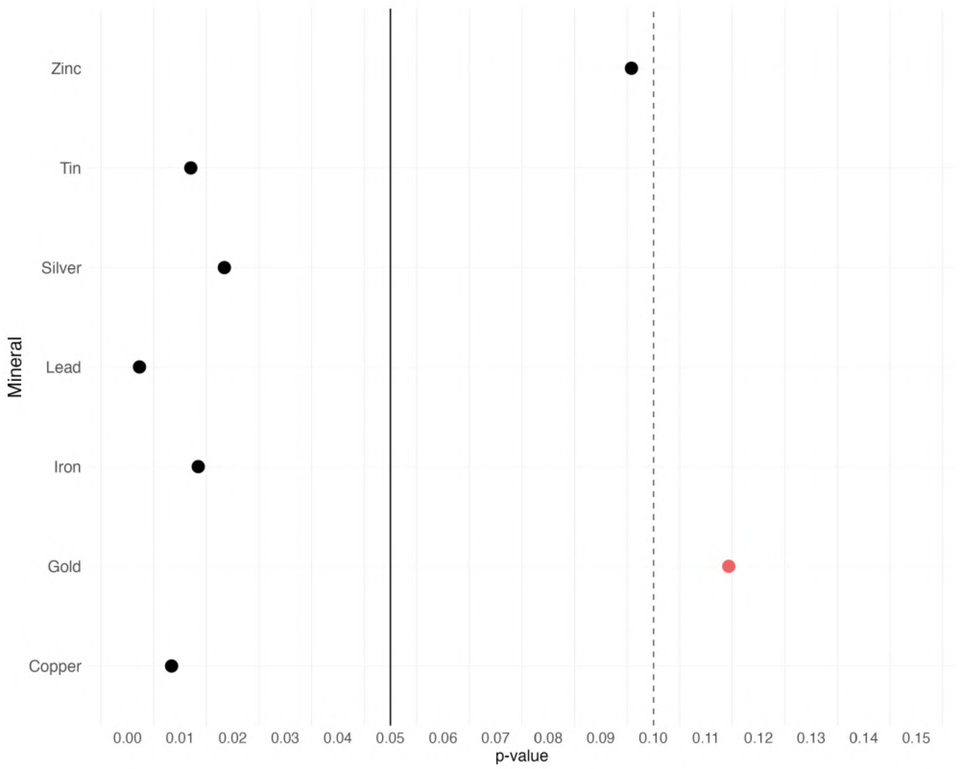

Notes: The p-values from Dickey–Fuller tests based on each mineral-specific *monthly* price series over the study period 2002–2019 are displayed. The null hypothesis is that the variable follows a random walk with nonzero drift. Price series have been purged of their common time components (i.e., I use the residuals from a regression of the log price on month × year dummies). The common certainty thresholds of 5% and 10% to reject the null hypothesis are depicted by the solid and dashed vertical lines, respectively.

Table B.7: First Difference – Main Mineral Price

	Force used against protesters			Protester behavior	
	Arrests	Injuries	Casualties	Violence	Riots
	(1)	(2)	(3)	(4)	(5)
$M \times \Delta$ ln(Price index)	0.0014	0.0028	0.0017*	-0.0007	-0.0005
	(0.0017)	(0.0021)	(0.0009)	(0.0013)	(0.0014)
District × year FEs	✓	✓	✓	✓	✓
Observations	94240	94240	94240	94240	94240

Notes: M equals one for mining districts (production or concessions) and 0 otherwise. Δ ln(Price) denotes the change in the natural logarithm of the main mineral price from month $t-1$ to t. The main mineral in a district is determined by the *(i)* total production value and *(ii)* count of a concession's primary commodities. Heteroskedasticity- and autocorrelation-corrected standard errors accounting for spatial correlation of up to 500 km and unlimited serial correlation are obtained with the Stata module `acreg` (Colella et al., 2023). A linear decay in distance in the spatial correlation structure is assumed. * $p < 0.1$, ** $p < 0.05$, *** $p < 0.01$.

Table B.8: First Difference – Price Index

	Force used against protesters			Protester behavior	
	Arrests	Injuries	Casualties	Violence	Riots
	(1)	(2)	(3)	(4)	(5)
$M \times \Delta$ ln(Price index)	0.0014	0.0029	0.0020**	-0.0005	-0.0005
	(0.0017)	(0.0022)	(0.0010)	(0.0013)	(0.0015)
District $\times$ year FEs	✓	✓	✓	✓	✓
Observations	94240	94240	94240	94240	94240

Notes: M equals one for mining districts (production or concessions) and 0 otherwise. Δ ln(Price index) denotes the change in the natural logarithm of the weighted price index from month $t-1$ to t. Weights are computed as each mineral's share of the *(i)* total production value or *(ii)* count of a concession's primary commodities. Heteroskedasticity- and autocorrelation-corrected standard errors accounting for spatial correlation of up to 500 km and unlimited serial correlation are obtained with the Stata module `acreg` (Colella et al., 2023). A linear decay in distance in the spatial correlation structure is assumed. * $p < 0.1$, ** $p < 0.05$, *** $p < 0.01$.

Table B.9: Spatial Lags

	Force used against protesters						Protester behavior			
	Arrests		Injuries		Casualties		Violence		Riots	
	(1)	(2)	(3)	(4)	(5)	(6)	(7)	(8)	(9)	(10)
$M\times$ ln(Price)	0.0002	0.0001	0.0024**	0.0020***	0.0008**	0.0006***	0.0000	0.0000	-0.0001	-0.0001
	(0.0002)	(0.0002)	(0.0011)	(0.0006)	(0.0004)	(0.0002)	(0.0001)	(0.0001)	(0.0002)	(0.0002)
$M\times$ ln(Price neighbors [1st degree])	0.0006	0.0004	-0.0012	-0.0031**	-0.0003	-0.0010*	0.0005*	0.0002	0.0007**	0.0006
	(0.0004)	(0.0003)	(0.0014)	(0.0013)	(0.0005)	(0.0005)	(0.0002)	(0.0002)	(0.0003)	(0.0004)
$M\times$ ln(Price neighbors [2nd degree])		0.0004		0.0036***		0.0013***		0.0004		0.0002
		(0.0003)		(0.0010)		(0.0004)		(0.0003)		(0.0004)
Cumulative effect	0.0007**	0.0009**	0.0012*	0.0026***	0.0005	0.0010***	0.0005	0.0006*	0.0006*	0.0006
	(0.0004)	(0.0004)	(0.0007)	(0.0008)	(0.0003)	(0.0003)	(0.0003)	(0.0004)	(0.0003)	(0.0004)
District $\times$ year FEs	✓	✓	✓	✓	✓	✓	✓	✓	✓	✓
Observations	93290	93290	93290	93290	93290	93290	93290	93290	93290	93290

Notes: M equals one for mining districts (production or concessions) and 0 otherwise. ln(Price) denotes the natural logarithm of the main mineral price in month t. The main mineral in a district is determined by the *(i)* total production value and *(ii)* count of a concession's primary commodities. Heteroskedasticity- and autocorrelation-corrected standard errors accounting for spatial correlation of up to 500 km and unlimited serial correlation are obtained with the Stata module `acreg` (Colella et al., 2023). A linear decay in distance in the spatial correlation structure is assumed. * $p < 0.1$, ** $p < 0.05$, *** $p < 0.01$.

Table B.10: Temporal Lags

	Force used against protesters									Protester behavior					
	Arrests			Injuries			Casualties			Violence			Riots		
	(1)	(2)	(3)	(4)	(5)	(6)	(7)	(8)	(9)	(10)	(11)	(12)	(13)	(14)	(15)
$M\times$ ln(Price $[t]$)	0.0014	0.0010	0.0014	0.0033	0.0034	0.0049	0.0019**	0.0020**	0.0036**	-0.0006	-0.0008	-0.0015	-0.0005	-0.0006	-0.0007
	(0.0017)	(0.0017)	(0.0025)	(0.0022)	(0.0023)	(0.0031)	(0.0009)	(0.0009)	(0.0017)	(0.0013)	(0.0013)	(0.0019)	(0.0014)	(0.0015)	(0.0020)
$M\times$ ln(Price $[t-1]$)	-0.0011	0.0016	0.0015	-0.0015	-0.0020	-0.0025	-0.0013	-0.0016	-0.0021	0.0009	0.0019	0.0020	0.0007	0.0013	0.0013
	(0.0017)	(0.0026)	(0.0027)	(0.0021)	(0.0031)	(0.0032)	(0.0009)	(0.0013)	(0.0014)	(0.0013)	(0.0019)	(0.0020)	(0.0015)	(0.0022)	(0.0023)
$M\times$ ln(Price $[t-2]$)		-0.0025	-0.0025		0.0005	0.0006		0.0003	0.0004		-0.0009	-0.0010		-0.0006	-0.0005
		(0.0016)	(0.0016)		(0.0018)	(0.0018)		(0.0008)	(0.0008)		(0.0008)	(0.0008)		(0.0010)	(0.0010)
$M\times$ ln(Price $[t+1]$)			-0.0003			-0.0012			-0.0014			0.0007			0.0001
			(0.0012)			(0.0017)			(0.0009)			(0.0007)			(0.0008)
Cumulative effect	0.0003*	0.0001	0.0001	0.0018**	0.0018**	0.0018**	0.0006**	0.0006**	0.0005*	0.0003*	0.0002*	0.0002**	0.0002	0.0002	0.0002
	(0.0002)	(0.0002)	(0.0002)	(0.0007)	(0.0008)	(0.0008)	(0.0003)	(0.0003)	(0.0003)	(0.0002)	(0.0001)	(0.0001)	(0.0002)	(0.0002)	(0.0001)
District $\times$ year FEs	✓	✓	✓	✓	✓	✓	✓	✓	✓	✓	✓	✓	✓	✓	✓
Observations	94240	94240	93744	94240	94240	93744	94240	94240	93744	94240	94240	93744	94240	94240	93744

Notes: M equals one for mining districts (production or concessions) and 0 otherwise. ln(Price) denotes the natural logarithm of the main mineral price in month t. The main mineral in a district is determined by the *(i)* total production value and *(ii)* count of a concession's primary commodities. Heteroskedasticity- and autocorrelation-corrected standard errors accounting for spatial correlation of up to 500 km and unlimited serial correlation are obtained with the Stata module `acreg` (Colella et al., 2023). A linear decay in distance in the spatial correlation structure is assumed. * $p < 0.1$, ** $p < 0.05$, *** $p < 0.01$.

B.4 Additional Robustness Checks

B.4.1 World Market Share

Table B.11: Sample of Districts with Negligible World Market Share

	Force used against protesters			Protester behavior	
	Arrests	Injuries	Casualties	Violence	Riots
	(1)	(2)	(3)	(4)	(5)
$M\times$ ln(Price)	0.0004**	0.0019**	0.0006**	0.0002	0.0002
	(0.0002)	(0.0007)	(0.0003)	(0.0002)	(0.0002)
District × year FEs	✓	✓	✓	✓	✓
Observations	90060	90060	90060	90060	90060

Notes: M equals one for mining districts (production or concessions) and 0 otherwise. Ln(Price) denotes the natural logarithm of the main mineral price in month t. The main mineral in a district is determined by the *(i)* total production value and *(ii)* count of a concession's primary commodities. Heteroskedasticity- and autocorrelation-corrected standard errors accounting for spatial correlation of up to 500 km and unlimited serial correlation are obtained with the Stata module `acreg` (Colella et al., 2023). A linear decay in distance in the spatial correlation structure is assumed. * $p < 0.1$, ** $p < 0.05$, *** $p < 0.01$.

B.4.2 Spatial Kernel

Table B.12: Alternative Levels of Spatial Clustering

	Force used against protesters			Protester behavior	
	Arrests	Injuries	Casualties	Violence	Riots
	(1)	(2)	(3)	(4)	(5)
$M\times$ ln(Price)	0.0004	0.0019	0.0007	0.0002	0.0002
distance: 50	(0.0002)**	(0.0007)***	(0.0003)***	(0.0002)	(0.0002)
distance: 100	(0.0002)*	(0.0007)***	(0.0003)***	(0.0002)	(0.0002)
distance: 250	(0.0002)**	(0.0007)***	(0.0003)**	(0.0002)	(0.0002)
distance: 500	(0.0002)**	(0.0007)***	(0.0003)**	(0.0002)	(0.0002)
distance: 750	(0.0002)**	(0.0007)***	(0.0003)**	(0.0002)	(0.0002)
distance: 1000	(0.0002)**	(0.0007)***	(0.0003)**	(0.0002)	(0.0002)
District $\times$ year FEs	✓	✓	✓	✓	✓
Observations	94240	94240	94240	94240	94240

Notes: M equals one for mining districts (production or concessions) and 0 otherwise. ln(Price) denotes the natural logarithm of the main mineral price in month t. The main mineral in a district is determined by the *(i)* total production value and *(ii)* count of a concession's primary commodities. Heteroskedasticity- and autocorrelation-corrected standard errors accounting for spatial correlation of up to the stated distance (in km) and unlimited serial correlation are obtained with the Stata module `acreg` (Colella et al., 2023). A linear decay in distance in the spatial correlation structure is assumed. * $p < 0.1$, ** $p < 0.05$, *** $p < 0.01$.

B.4.3 Multiple Hypothesis Correction

Table B.13: Romano–Wolf (Multiple Hypothesis Testing–Adjusted) P-Values

	Outcome	Model p-value	Resampled p-value	Romano-Wolf p-value
Force used against protesters	Arrests	0.045	0.008	0.088
	Injuries	0.010	0.044	0.088
	Casualties	0.011	0.074	0.088
Protester behavior	Violence	0.220	0.172	0.172
	Riots	0.343	0.100	0.112

Notes: The Romano–Wolf p-values adjusted for multiple hypothesis testing are calculated with the resampled null distribution from 500 bootstrap samples with the *Stata* command `rwolf` (Clarke et al., 2020).

Figure B.2: Null Distributions and Original T Statistics

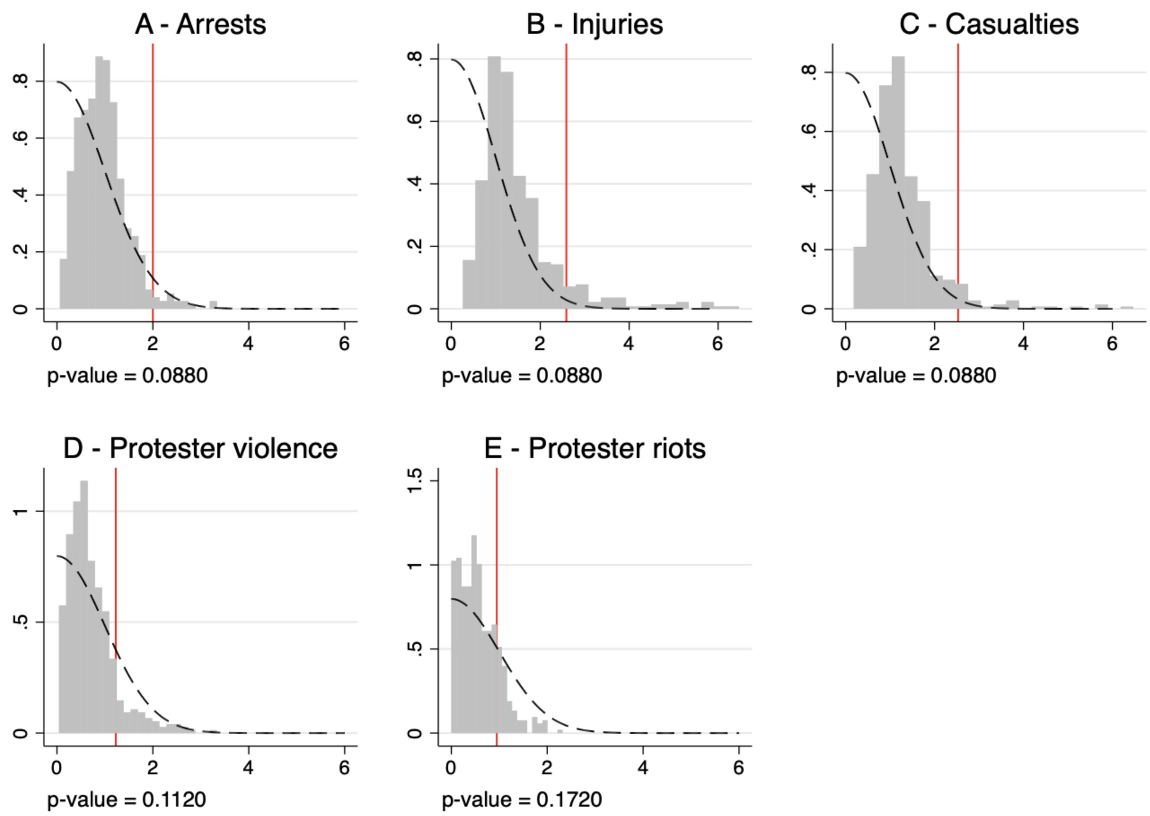

Notes: Each panel documents the null distributions used for the calculation of the *Romano–Wolf* adjusted p-values for each of the 5 baseline dependent variables. The Romano–Wolf adjusted p-values are calculated with the *Stata* command `rwolf` (Clarke et al., 2020) and displayed below each panel. The histogram in each panel depicts the stepdown resampled null distribution from 500 bootstrap samples. The dashed line captures the theoretical half-normal, and the solid vertical line presents the original t statistic corresponding to each outcome.

C Democracy, Corruption, and Violence

C.1 Manipulation Test

Figure C.1: Manipulation Test

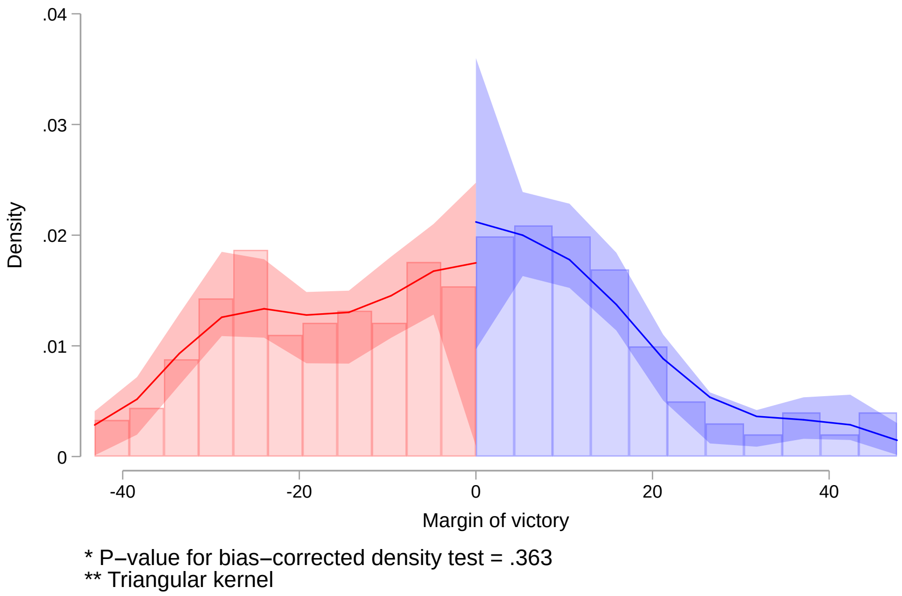

Notes: This figure presents the manipulation test suggested by Cattaneo et al. (2018) and implemented in the Stata command `rddensity` using a quadratic polynomial and triangular kernel weights. The p-value for the bias-corrected density test is 0.36. The p-values using a polynomial of degrees 1 and 3 are 0.38 and 0.54, respectively.

C.2 RDD Tables

Table C.1: Smooth Covariates near Cut-off

	Obs. (1)	Mean (2)	Std. dev. (3)	Coef. (4)	Std. error (5)	p-value (6)	Effect. obs. (7)
A. Individual covariates							
Women	234	0.051	0.221	0.062	0.087	0.557	131
B. Political covariates							
Political competition	233	4.788	1.491	-0.792	0.692	0.233	102
Canon minero	230	0.960	3.837	-0.178	0.610	0.299	69
Royalties	230	0.315	1.423	-0.105	0.430	0.967	50
C. Other municipality socioeconomic characteristics							
Nighttime lights	229	2.277	3.605	-1.339	1.076	0.143	92
Area	233	702.819	1465.260	6.530	278.685	0.686	79
Elevation	233	3420.060	1194.684	339.718	452.793	0.579	112
Population density	233	28.955	110.916	-41.249	19.851	0.072	87
Total population	234	8754.526	11000.000	-577.203	3437.225	0.890	73
Indigenous population density	233	0.001	0.006	-0.004	0.005	0.317	140
Road density	233	0.058	0.084	-0.007	0.032	0.728	107
River density	233	0.267	0.075	-0.017	0.048	0.621	154
Proportion of native land	233	0.002	0.012	-0.008	0.009	0.321	140
Proportion of indigenous land	233	0.000	0.000	0.000	0.000	0.946	74
Proportion of lakes	233	0.004	0.012	0.006	0.005	0.159	108

Notes: The first three columns present the basic statistics for the entire sample (total number of observations, mean, and standard deviation) of each covariate. Column 4 reports the RDD's point estimate of the effect of a pro-mining candidate victory on each covariate (as the dependent variable). Following Cattaneo et al. (2020), the MSE-optimal bandwidth is calculated for each covariate. Bias-corrected robust standard errors adjusted for clustering at the regional level are reported in column 5. Column 6 reports the estimated p-value, and the number of effective observations is detailed in column 7.

Table C.2: Pro-Mining Local Politicians and Corruption and Police Violence during Term in Office

	Police Violence		Corruption case		Case at stage 1		Case at stage 2 or 3	
	(1)	(2)	(3)	(4)	(5)	(6)	(7)	(8)
Police violence	0.129	0.159	-0.227	-0.212	-0.341**	-0.369*	0.150	0.160
Cluster-robust p-value	0.126	0.128	0.149	0.455	0.020	0.095	0.295	0.296
90% CI	[-0.012, 0.331]	[-0.014, 0.375]	[-0.598, 0.039]	[-0.635, 0.238]	[-0.609,-0.104]	[-0.774,-0.006]	[-0.076, 0.344]	[-0.092, 0.414]
No. of obs.	234	234	234	234	234	234	234	234
Bandwidth obs.	85	138	97	124	134	126	86	121
Dep. var. mean	0.08	0.08	0.38	0.38	0.23	0.23	0.16	0.16
Effect mean (%)	159.26	196.30	-58.96	-55.06	-150.88	-163.27	94.94	101.27
Bandwidth (left/right)	{7.9; 11}	{15.1; 21}	{12.8; 11}	{15.4; 15}	{15.4; 19}	{15.2; 16}	{9.2; 10}	{11.4; 18}
(Local) polynomial order	1	2	1	2	1	2	1	2

Notes: Even columns present local linear estimates of average treatment effects at the cut-off estimated with triangular kernel weights and MSE-optimal bandwidth. Odd columns present quadratic estimates of average treatment effects at the cut-off estimated with triangular kernel weights and MSE-optimal bandwidth. Ninety percent robust confidence intervals and p-values adjusted for clustering at the state level are computed following Calonico et al. (2014). Bandwidth obs. denotes the number of observations in the MSE-optimal bandwidth. The effect size (%) is computed as the point estimate over the dependent variable mean × 100. * $p < 0.1$, ** $p < 0.05$, *** $p < 0.01$.

D Dynamic Causal Inference

D.1 Technical Appendix

D.1.1 Marginal Structural Models

Using the set-up introduced in Section with $i = 1, ..., N$ social conflicts, each spanning $t = 1, ..., T_i$ 3-month periods, where in each time period of the conflict local authorities decide to use excessive force against protesters ($A_{it} = 1$) or not ($A_{it} = 0$), let $\underline{a}_t \equiv (a_1, ..., a_t)$ be the realized action sequence of A_{it} (e.g., $a_3 = \{a_1 = 0; a_2 = 1; a_3 = 0\}$) and $\underline{a}$ a *representative* history of excessive force use. Each *representative* history $\underline{a}$ is associated with a different potential outcome $Y(\underline{a})$. Consequently, there exist 2^T different potential action sequences $\underline{a}$ and potential outcomes, but we observe only one realization for each conflict. The remaining potential outcomes are counterfactuals. Marginal structural models (MSMs) break this curse of dimensionality by assuming a *parametric* form for the mean of the potential outcome:

$$E\left[Y\left(\underline{a}\right)\right] = g\left(\underline{a}; \beta\right) \tag{D.1}$$

while leaving the rest of the distribution of $Y(\underline{a})$ unspecified (Blackwell, 2013). Intuitively, MSMs assume that "similar" actions lead to "similar" outcomes.

The challenge is that, if there exist omitted variables that affect both treatment and outcome, simply controlling for them in standard regression models will not lead to unbiased estimates if the the time-varying confounders are themselves affected by past actions (*post-treatment bias*). Fortunately, Robins et al. (2000) show that, under the assumptions of sequential ignorability ("no unmeasured confounders") and positivity, estimating an *inverse probability of treatment reweighted version* of (D.1) will recover the unbiased (treatment) effect. The (*unstabilized*) inverse probability of treatment weights (IPTW) in each time period are defined as[40]:

$$W_{it} = \frac{1}{\Pr\left(A_{it} | \underline{A}_{it-1}, \underline{X}_{it}.\right)} \tag{D.2}$$

The overall weight for each social conflict is then calculated as:

$$W_i = \prod_{t=1}^{T} W_{it}. \tag{D.3}$$

A common approach of modeling the probability of police violence is to estimate a

[40]For the stabilized version of the IPTW, please refer to equation (4).

logit model:

$$\Pr\left(A_{it}=1|\underline{A}_{it-1},\underline{X}_{it}\right)=\left[1+\exp\left\{-h\left(\underline{A}_{it-1},\underline{X}_{it}\right)\right\}\right]^{-1}, \tag{D.4}$$

where h is a linear additive function of the action and covariate history.

Two common forms of the linear additive function of the MSM in either a logit or a linear probability model are:

$$\text{logit}^{-1}\Pr\left(y_i=1|\underline{A}_i,\underline{X}_i)\right)=y_i=\beta_0+\beta_1\left(\sum_{t=1}^{T}A_{it}\right)+\beta_2X_{i1} \tag{D.5}$$

$$\text{or}\qquad \text{logit}^{-1}\Pr\left(y_i=1|\underline{A}_i,\underline{X}_i)\right)=y_i=\beta_0+\beta_1\mathbf{1}_{\sum_{t=1}^{T}A_{it}>0}+\beta_2X_{i1}, \tag{D.6}$$

where $\mathbf{1}_{\sum_{t=1}^{T}A_{it}>0}$ is a binary indicator that equals one if any police violence was observed during social conflict i and $\sum_{t=1}^{T}A_{it}$ is equal to the total number of time periods with at least one incident of police violence over the course of the conflict; X_{i1} is the set of baseline covariates prior to the start of the conflict and comprises all baseline covariates considered in the standard IPTW logit model (see Table D.1).

D.1.2 LASSO

I estimate inverse probability weights using a *LASSO-logit* function, which predicts treatment using the following penalized model:

$$\hat{\beta}=\arg\min_{\beta}\left(-\underbrace{\left[\frac{1}{N}\sum_{i=1}^{N}y_{it}\times\left(X_{it}^{T}\beta\right)-\log\left(1+e^{X_{it}^{T}\beta}\right)\right]}_{\text{logit}}+\underbrace{\lambda\sum_{j=1}^{p}|\beta_j|}_{\text{lasso penalty}}\right), \tag{D.7}$$

where y_{it} is the binary indicator for police violence and $lambda$ is the is the penalty weight applied to the coefficient values for each standardized variable in the covariate matrix X_{it} comprising all potential predictors of police violence. I use the `glmnet` (Friedman et al., 2010) **R** package to implement the LASSO-logit model.

The optimal value of λ (λ^*) is identified to minimize the out-of-sample logarithmic loss using 10-fold cross-validation repeated 10 times.[41] Application of oversampling algorithms such as ROSE (Menardi and Torelli, 2014; Lunardon et al., 2014) and SMOTE (Chawla et al., 2011) to address the class imbalance in the data did not improve the out-of-sample fit of the LASSO-logit model and are not reported.

I compute the probability of police violence for each social conflict as the predicted

[41]The repetitions ensure that the stochasticity in the 10-fold cross-validation split does not significantly affect the results. I use the `vfold_cv` function of the `tidymodels` (Kuhn and Wickham, 2020) **R** package to implement the k-fold cross-validation.

value from the fitted coefficients $\hat{\beta}$ at λ^*.

D.1.3 Gradient Boosting Machines

Gradient boosting machines (GBM) are among the most popular machine learning algorithms. In contrast to *random forest*, GBM builds trees *sequentially* and not *independently* such that each new tree improves the predictive power of the the ensemble of trees. Intuitively, GBM *boosts* its performance by sequentially building new trees that specifically try to correct poorly predicted observations in previous trees.

Formally, at each stage m, *boosting* solves:

$$\hat{\Theta}_m = \arg\min_{\Theta_m} \sum_{i=1}^{N} L\left(y_i, f_{m-1}(X_1) + T_m(X_i;\Theta_m)\right), \tag{D.8}$$

where $f_{m_1}(X_i)$ is the value of the sum of trees that was estimated in the first $m-1$ stages (Montgomery and Olivella, 2018). GBM provides an accurate and fast approximation of the optimization problem in (D.8). Specifically, GBM fits a new tree to the *negative gradient* of the loss function $-\mathbf{g}_m$, i.e.,

$$\hat{\Theta}_m = \arg\min_{\Theta_m} \sum_{i=1}^{N} L\left(-g_{im} - T_m(X_i;\Theta_m)\right)^2, \tag{D.9}$$

where g_{im} is the i_{th} component of $\mathbf{g}_m$. Let $\mathbf{g}_m = \delta L\left(y_i, f_{m-1}(X_1)\right)/\delta f_{m-1}(X_1$ be the gradient of the loss function at stage m; then, $\mathbf{g}_m$ is a vector pointing in the direction of the *most steeply increasing loss* (Montgomery and Olivella, 2018). Intuitively, the optimal path for a skier to win the race is to choose the path with the steepest slope.

One of the key parameters in gradient descent is the size of the steps, which is controlled by the *learning rate*. On the one hand, if the chosen learning rate is too small, then the algorithm will take many steps to find the minimum, increasing computation time. On the other hand, if the chosen learning rate is too high, the algorithm might miss the *global* minimum, negating efficiency gains in computation time. Moreover, if the loss function is not *convex*, the algorithm might end up at a *local* minimum or plateau in lieu of the *global* minimum. *Stochastic gradient descent* addresses the latter by growing the next tree using a randomly drawn subsample of the training data. While the stochasticity does not allow the algorithm to reach the *absolute* global minimum, it is less susceptible to local minimums or plateaus.

The following paragraph discusses the main hyperparameters for tuning the extreme gradient boosting (XGBoost) algorithm (Chen and Guestrin, 2016) made available in the `tidymodels` (Kuhn and Wickham, 2020) **R** package, an optimized gradient boosting library that allows the user to set additional hyperparameters to avoid overfitting or account for class imbalance.

scale_pos_weight Balance the positive and negative weights. Value set to recommended sum of majority class instances divided by sum of minority class instances.[42]

trees Reports the total number of trees in the sequence.

tree_depth Controls the depth of the individual trees. Smaller trees are computationally efficient and less prone to overfitting but may miss important variable interactions.

min_n Reports the minimum number of observations in terminal nodes. Higher values safeguard against overfitting, but lower values can be beneficial in imbalanced datasets.

loss_reduction Specifies a minimum loss reduction required to make a further partition on a leaf node of the tree.

mtry Subsampling of predictors in every boosting iteration. Higher values are beneficial if there are fewer relevant predictors or strong multicollinearity.

sample_size Conducts random sampling of rows for each tree in the sequence. Higher values reduce overfitting.

learn_rate Determines the contribution of each tree to the final outcome and controls how quickly the algorithm proceeds down the gradient descent.

The optimal hyperparameter combination is identified to minimize the out-of-sample logarithmic loss using 10-fold cross-validation. To allow an efficient search for the appropriate set of tuning parameters, the 10-fold cross-validation is repeated 5 times, and I use a *space-filling* Latin hypercube grid search design implemented with the `grid_latin_hypercube` function of the `dials` **R** library covering 250 parameter value combinations. Intuitively, the Latin hypercube design finds a configuration of points that covers the parameter space with the smallest chance of overlapping.

[42] `https://xgboost.readthedocs.io/en/latest/tutorials/param_tuning.html`.

D.1.4 Covariates Included in Predictive Models of Police Violence

Table D.1: Covariates included in Predictive Models of Police Violence

Variable description	Type	Frequency	GLM	LASSO	XGBoost
Time-varying					
Police violence$_{t-1}$	Binary	Period	✓	✓	✓
Police violence$_{t-2}$	Binary	Period	✓	✓	✓
Police violence$_{t-3}$	Binary	Period	✓	✓	✓
Protest$_{t}$	Binary	Period	✓	✓	✓
Protest$_{t-1}$	Binary	Period	✓	✓	✓
Protest$_{t-2}$	Binary	Period	✓	✓	✓
Protest$_{t-3}$	Binary	Period	✓	✓	✓
Protester riots$_{t}$	Binary	Period	✓	✓	✓
Protester riots$_{t-1}$	Binary	Period	✓	✓	✓
Protester riots$_{t-2}$	Binary	Period	✓	✓	✓
Protester riots$_{t-3}$	Binary	Period	✓	✓	✓
Crop price$_{t}$	Continuous	Period		✓	✓
Crop price$_{t-1}$	Continuous	Period		✓	✓
Crop price$_{t-2}$	Continuous	Period		✓	✓
Precipitation$_{t}$	Continuous	Period		✓	✓
Precipitation$_{t-1}$	Continuous	Period		✓	✓
Precipitation$_{t-2}$	Continuous	Period		✓	✓
Mineral price$_{t}$	Continuous	Period	✓	✓	✓
Mineral price$_{t-1}$	Continuous	Period	✓	✓	✓
Mineral price$_{t-2}$	Continuous	Period		✓	✓
Temperature$_{t}$	Continuous	Period		✓	✓
Temperature$_{t-1}$	Continuous	Period		✓	✓
Temperature$_{t-2}$	Continuous	Period		✓	✓
Conflict length	Discrete	Period	✓	✓	✓
Relative time period	Discrete	Period	✓	✓	✓
Relative time period × Conflict length	Discrete	Period	✓	✓	✓
Log(Canon minero)$_{t-1}$	Continuous	Year		✓	✓
Log(Royalties)$_{t-1}$	Continuous	Year		✓	✓
Night Lights$_{t-1}$	Continuous	Year		✓	✓
Year	Nominal	Year	✓	✓	✓

Table D.1: Covariates included in predictive models of police violence *(continued)*

Variable description	Type	Frequency	GLM	LASSO	XGBoost
Baseline					
Indigenous	Binary	Constant	✓	✓	✓
Canon minero	Continuous	Constant		✓	✓
Elevation	Continuous	Constant		✓	✓
Leverage	Continuous	Constant		✓	✓
Log(Canon minero)	Continuous	Constant		✓	✓
Log(Market value)	Continuous	Constant		✓	✓
Log(Population)	Continuous	Constant		✓	✓
Log(Royalties)	Continuous	Constant		✓	✓
Log(Size)	Continuous	Constant		✓	✓
Market value	Continuous	Constant		✓	✓
Night light density	Continuous	Constant		✓	✓
Night lights	Continuous	Constant		✓	✓
Indigenous area (%)	Continuous	Constant		✓	✓
Native area (%)	Continuous	Constant		✓	✓
Lake area (%)	Continuous	Constant		✓	✓
Population density	Continuous	Constant		✓	✓
Indigenous population density	Continuous	Constant		✓	✓
River density	Continuous	Constant		✓	✓
Road density	Continuous	Constant		✓	✓
Royalties	Continuous	Constant		✓	✓
Majority owner location	Nominal	Constant	✓	✓	✓
Altitude	Nominal	Constant	✓	✓	✓
Canon minero	Nominal	Constant	✓	✓	✓
Elevation	Nominal	Constant	✓	✓	✓
Leverage	Nominal	Constant	✓	✓	✓
Market capitalization	Nominal	Constant	✓	✓	✓
Market value	Nominal	Constant	✓	✓	✓
Night light density	Nominal	Constant	✓	✓	✓
Night lights	Nominal	Constant	✓	✓	✓
Indigenous area (%)	Nominal	Constant	✓	✓	✓
Native area (%)	Nominal	Constant	✓	✓	✓
Lake area (%)	Nominal	Constant	✓	✓	✓
Population	Nominal	Constant	✓	✓	✓
Population density	Nominal	Constant	✓	✓	✓

Table D.1: Covariates included in predictive models of police violence *(continued)*

Variable description	Type	Frequency	GLM	LASSO	XGBoost
Indigenous population density	Nominal	Constant	✓	✓	✓
River density	Nominal	Constant	✓	✓	✓
Road density	Nominal	Constant	✓	✓	✓
Royalties	Nominal	Constant	✓	✓	✓
Size	Nominal	Constant	✓	✓	✓

D.2 Model Performance

Table D.2 presents the out-sample fit statistics for the three algorithms under consideration. Fit statistics are calculate on 20% of the original data set.[43] The first three columns show that the predictions are highly correlated across models. Figure D.1 corroborates this assertion. The predicted probabilities across algorithms exhibit comparable distributions for both true positives and true negatives. However, small differences in predictions can have substantial effects on the distribution of final weights (see Figure 4). Furthermore, while the predicted probabilities seem to be well behaved for true negatives with the probability mass close to 0 across algorithms, the predictions for true positives show more variations across algorithms. Visual inspection of the probability distributions for true positives and negatives for each algorithm suggests that the LASSO-logit model provides the best results avoiding extreme values. This observation is substantiated with the LASSO-logit model having the lowest *Brier score* and *log loss* (cross-entropy loss); the two statistics using probabilities as opposed to class labels—as in the the case of *balanced accuracy* and the *area under the receiver operator curve* (AUC ROC)—to measure the fit of the model.

[43]The original split of the data in training and test set uses stratified sampling to account for the imbalance in the data set.

Table D.2: Predictive Out-of-Sample Fit Statistics for Competing Models

	Pairwise correlation			Out-of-sample fit statistics			
	GLM	LASSO	XGBoost	Balanced accuracy	Brier score	AUC ROC	Log loss
GLM	1.000	0.591	0.515	0.594	0.030	0.717	0.370
LASSO	0.591	1.000	0.535	0.500	0.022	0.655	0.108
XGBoost	0.515	0.535	1.000	0.594	0.028	0.564	0.134

Notes: Predictive fit statistics for the logistic regression model (GLM), LASSO-logit model (Lasso), and gradient boosting machine are presented using 20% from the original dataset that was left out of the training process. Higher values for the balanced accuracy score (Bal. Accuracy) and the area under the receiver operator curve (AUC ROC) indicate superior fit. Lower values for the Brier score and the logarithmic loss (log loss) indicate superior fit.

Figure D.1: Distribution of Predicted Probabilities

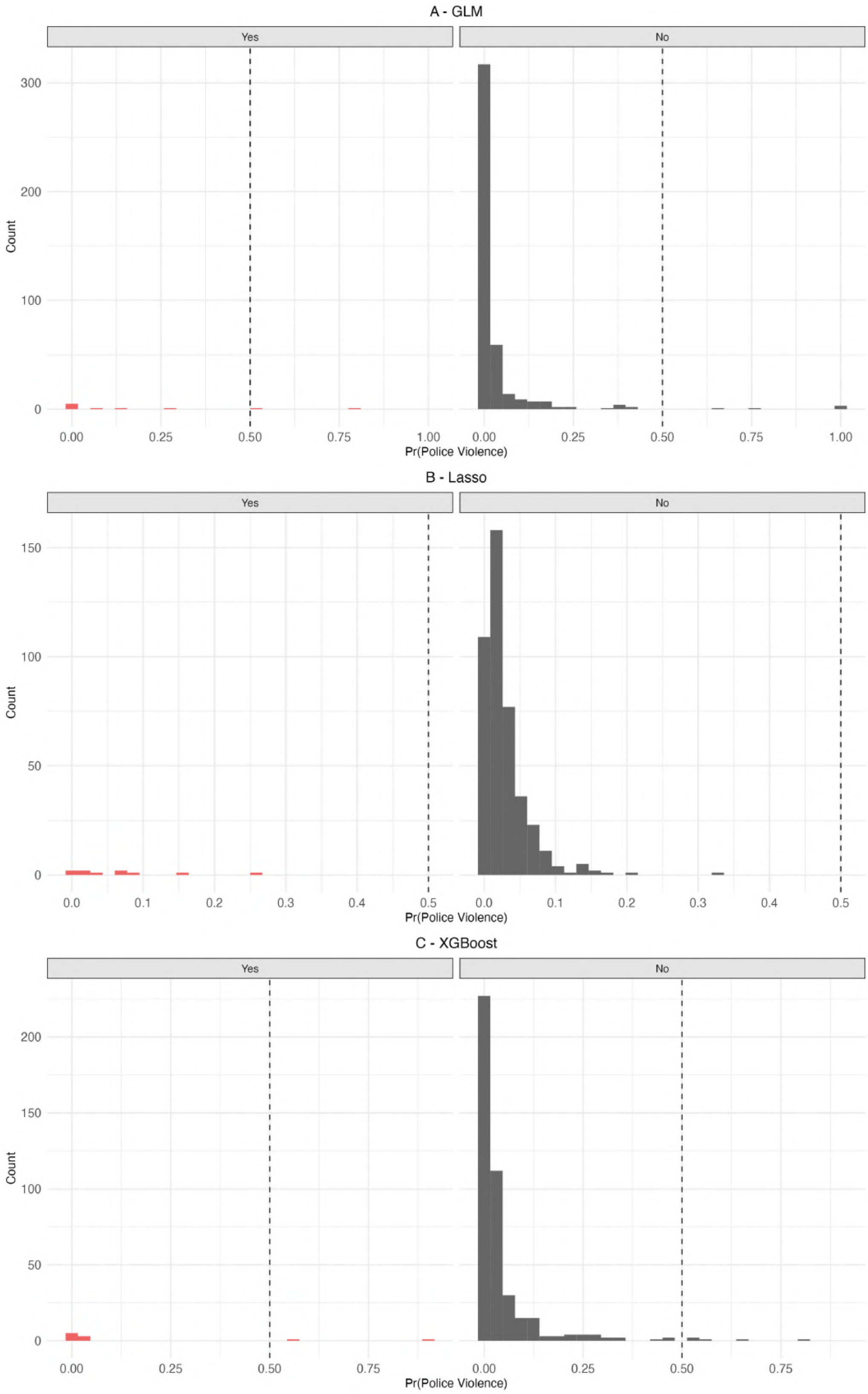

Notes: The distribution of predicted probabilities for 20% of the original data set left out during the training process across algorithms is displayed with the left, respectively right panel presenting predicted probabilities for true positives (Yes) and true negatives (No).

D.3 Directed Acyclic Graphs (DAGs)

Figure D.2: Dynamic Causal Inference

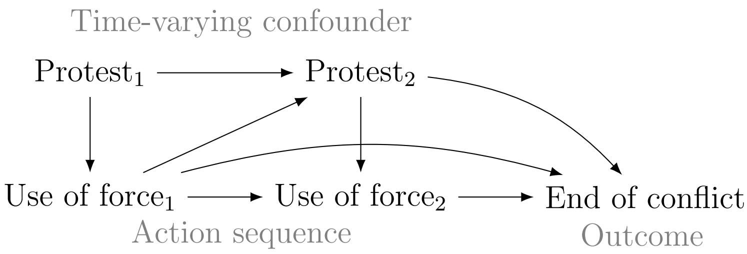

Notes: Each arrow represents a causal relationship.

Figure D.3: Sequential Ignorability Assumption

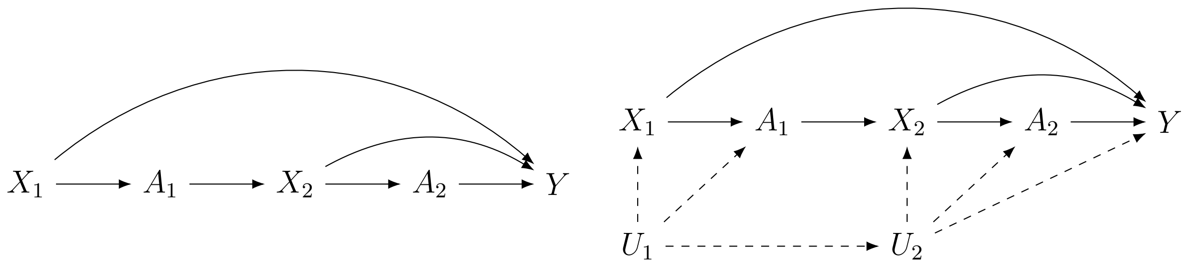

(a) Sequential ignorability holds.

(b) Sequential ignorability fails to hold.

Appendix References

Blackwell, M. (2013). A framework for dynamic causal inference in political science. *American Journal of Political Science*, 57(2):504–520.

Cardellino, C. (2019). Spanish Billion Words Corpus and Embeddings.

Chawla, N. V., Bowyer, K. W., Hall, L. O., and Kegelmeyer, W. P. (2011). Smote: Synthetic minority over-sampling technique. *The Journal of artificial intelligence research*, 16:321–357.

Chen, T. and Guestrin, C. (2016). Xgboost: A scalable tree boosting system. In *Proceedings of the 22nd ACM SIGKDD International Conference on Knowledge Discovery and Data Mining*, KDD '16, page 785–794, New York, NY, USA. Association for Computing Machinery.

Clarke, D., Romano, J. P., and Wolf, M. (2020). The Romano–Wolf multiple-hypothesis correction in Stata. *Stata Journal*, 20(4):812–843.

Colella, F., Lalive, R., Sakalli, S. O., and Thoenig, M. (2023). acreg: Arbitrary correlation regression. *Stata Journal*, 23(1):119–147.

Friedman, J., Tibshirani, R., and Hastie, T. (2010). Regularization paths for generalized linear models via coordinate descent. *Journal of Statistical Software*, 33(1):1–22.

Harris, I., Osborn, T. J., Jones, P., and Lister, D. (2020). Version 4 of the CRU TS monthly high-resolution gridded multivariate climate dataset. *Scientific data*, 7(1):109.

Honnibal, M., Montani, I., Van Landeghem, S., and Boyd, A. (2020). spaCy: Industrial-strength Natural Language Processing in Python.

Kuhn, M. and Wickham, H. (2020). *Tidymodels: a collection of packages for modeling and machine learning using tidyverse principles.*

Lunardon, N., Menardi, G., and Torelli, N. (2014). ROSE: a Package for Binary Imbalanced Learning. *The R Journal*, 6(1):79–89.

Menardi, G. and Torelli, N. (2014). Training and assessing classification rules with imbalanced data. *Data mining and knowledge discovery*, 28(1):92–122.

Monfreda, C., Ramankutty, N., and Foley, J. A. (2008). Farming the planet: 2. Geographic distribution of crop areas, yields, physiological types, and net primary production in the year 2000. *Global Biogeochemical Cycles*, 22(1).

Montgomery, J. M. and Olivella, S. (2018). Tree-based models for political science data. *American Journal of Political Science*, 62(3):729–744.